POLITECNICO DI TORINO

SCUOLA DI DOTTORATO
Dottorato in Ingegneria Aerospaziale – XXV ciclo

Tesi di Dottorato

Cooperative Deployment of satellite formation into Highly Elliptic Orbit

Francesco Simeoni
SSD ING-IND/03

Tutore
prof. Lorenzo Casalino

Aprile 2013

Acknowledgements

This work was supported by the Centre National d'Etudes Spatiales (CNES), [Contract Number 93333/00].

Thanks to prof. Lorenzo Casalino for guiding me in this long trip and for the great patience.

Thanks to prof. Guido Colasurdo, prof. Dario Pastrone and Alessandro Zavoli for the work made and for the achievements reached together.

Thanks to Richard Epenoy for his supervising.

Thanks to Nathan Strange and all the JPL guys.

Grazie alla mia famiglia e ad ai miei amici per essere sempre presenti.

Contents

Acknowledgements I

1 Indirect method applied to complex problems **5**
1.1 Trajectory optimization of satellite deployment 5
1.2 Case study: Simbol-X 9

2 Methods for trajectory optimization **13**
2.1 Optimization problem: definition and taxonomy 13
2.2 Direct Algorithms 16
2.3 Evolutionary Algorithms 21
2.3.1 Genetic Algorithm 22
2.3.2 Differential Evolution 23
2.3.3 Particle Swarm Optimization 23
2.3.4 Ant Colony Optimization 24
2.3.5 Branch and Bound 24
2.3.6 Simulated Annealing 24
2.3.7 Cooperative hybrid algorithm 25
2.4 Indirect Method Optimization 26

3 Dynamic Model **35**
3.1 Differential equations and reference frame 35
3.2 Geopotential Model 40
3.3 N-body perturbations 46
3.4 Solar Radiation pressure 50

4 Case study: Cooperative deployment **52**
4.1 Mission in HEO: Simbol-X 52
4.2 Optimal values of the control 55
4.3 Single satellite optimal control 56
4.4 Formation Flight 59
4.4.1 Chaser Target 60

4.4.2 Cooperative strategy 61
4.5 Collision Avoidance 63
4.6 Optimal Constant-Direction Thrust 65
4.7 Errors in control law 67

5 Numerical Results **70**
5.1 Single Satellite Deployment 70
5.1.1 J2 solutions 71
5.1.2 Luni-Solar perturbations 75
5.1.3 Example Case Analysis 80
5.2 Chaser-Target and Cooperative deployment 82
5.3 Collision Avoidance 85
5.4 Optimal Constant-Direction Thrust 90
5.5 Errors in control law 92

A Ringraziamenti finali e Aknowledgements **101**

Bibliography **104**

List of Tables

4.1 Initial and final orbit characteristics. 53
4.2 Satellites Properties. 53
5.1 Time and angular length of each burn (J2 only). 73
5.2 Characteristics of the 4.5-rev. transfer with departure on Dec. 1, 2015. 80
5.3 Performance for different deployment strategies (J2 model, 1 N thrust). 84
5.4 Final mass comparison with different control laws for SAT0 deployment. 91
5.5 Optimal thrust angles for departure on December 2, 2015. 92
5.6 Optimal thrust angles for departure on December 25, 2015. 92

List of Figures

1.1 Artistic Impression of Simbol-X. Credit: CNES 9
1.2 Distance between satellite: the left satellite is the detector and the satellite on the right is the mirror. Credit: CNES 10
1.3 Viewing direction. Credit: CNES 11
3.1 Spherical Reference frame 38
3.2 Thrust Direction 41
3.3 Image of Geoid. Credit: Grace/NASA 42
3.4 Schematic geometry of gravitational perturbations 47
3.5 Schematic geometry of the Earth shadow 51
5.1 Trajectory plot 71
5.2 Comparison between mission with different number of revolutions using 1N or 8N thrust level 72
5.3 r_p and r_a during a 2.5-revolution mission, 8N thrust 74
5.4 r_p and r_a during a 4.5-revolution mission, 8N thrust 74
5.5 r_p and r_a during a 2.5-revolution mission, 1N thrust 75
5.6 Final mass with departure date along 2016 76
5.7 Final mass and switching function from December 2015 to February 2016 76
5.8 Lunar perturbations on final mass considering Moon position fixed . . 78
5.9 Lunar perturbations on final mass considering Moon motion 78
5.10 Spacecraft right ascension ϑ deg 79
5.11 Total mass [kg] of the two satellites deployed individually 80
5.12 SAt0 Switching structure 81
5.13 Thrust angles of 4.5-revolution mission 81
5.14 Final orbital elements 82
5.15 Thrust profile. On the top: time t. In the bottom: adimensional time ϵ 83
5.16 Switching Function SAT1 83
5.17 Switching Function SAT2 84
5.18 Switching function SAT1. Total final mass with departure date along 2016 86

5.19 Switching function SAT2. Total final mass with departure date along 2016 86
5.20 Energy of SAT1 and SAT2 with J2 perturbations only 87
5.21 Inter-satellite distance 10 December 2015 88
5.22 Inter-satellite distance 10 December 2015, magnification 89
5.23 Inter-satellite distance 2 December 2015 89
5.24 Inter-satellite distance 2 December 2015, magnification with switching points 89
5.25 Inter-satellite distance 2 December 2015, magnification 90
5.26 r_a SAT1 dispersion 93
5.27 r_a SAT2 dispersion 93
5.28 r_p SAT1 dispersion 94
5.29 r_p SAT2 dispersion 94
5.30 Final phasing time dispersion 95
5.31 Re-optimization Scheme 95
5.32 Observation points in mission timeline 96
5.33 Comparison between PAAA and PAA0 solutions 98

Abstract (English)

Space trajectory optimization and mission design analysis have not general standards and procedures suitable for any kind of problems. Methods and results improve thanks the progress in computer science, numerical analysis, and engineering.

The aim of this thesis is to enlarge the field of application of indirect optimization methods, which are based on the theory of optimal control, to trajectory optimization problems characterized by a complex dynamical model, which considers Earth oblateness, gravitational perturbations from Moon and Sun, and solar radiation pressure.

The case study is the finite-thrust deployment of a two-satellite formation into a highly elliptic orbit. The optimization procedure provides the engine switching times and the thrust direction during each burn in order to transfer the satellites to the same prescribed final orbit with assigned distance between them at the apogee passage; the total final mass is maximized.

A minimum-distance constraint is introduced when required to avoid collision risk. Different deployment strategies are analyzed; in particular, the classical chaser-target approach is compared to cooperative deployment. Necessary conditions for optimality corresponding to the different strategies are derived and numerical results presented. The optimal solution exhibits remarkable changes depending on the departure date, and a procedure has been developed to assure convergence with the use of a single tentative solution.

The same problem was also solved using a suboptimal control law with thrust angles that remain constant in the inertial frame during each thrust arc. A preliminary study for considering errors introduced by thrust dispersion was carried on. The use of a re-optimization procedure after each apogee burn allows for a remarkable reduction of the errors on the final orbit achievement both in the single satellite case and in the formation deployment. In particular, intrinsically robust deployment strategies, characterized by a short final burn, have been identified.

Abstract (Italiano)

L'ottimizzazione di traiettorie spaziali e l'analisi di missione non possiedono al momento procedure e standard adatti ad ogni genere di problema. Metodi e risultati migliorano grazie ai progressi nell'informatica, nell'analisi numerica e nell'ingegneria. Lo scopo di questa tesi è di allargare il campo di applicazione dei metodi indiretti, che sono basati sulla teoria del controllo ottimale, a problemi di ottimizzazione di traiettorie caratterizzati da un modello dinamico complesso, che consideri la non sfericità della Terra, le perturbazioni gravitazionali della Luna e del Sole e la pressione di radiazione solare. Il caso studiato è il dispiegamento in orbita di una formazione di due satelliti in un'orbita altamente ellittica (HEO: Highly Elliptic Orbit) con spinta finita. La procedura di ottimizzazione fornisce i tempi di accensione e spegnimento del motore e la direzione di spinta durante ogni sparo, in modo tale da trasferire i satelliti sulla stessa orbita finale con una distanza assegnata al passaggio all'apogeo; la massa totale dei due satelliti alla fine del trasferimento è l'indice di prestazione massimizzato.

Un vincolo di distanza minima è introdotto quando necessario per evitare il rischio di collisione. Diverse strategie per il dispiegamento della formazione sono state analizzate; in particolare, il classico approccio chaser-target è stato comparato al dispiegamento cooperativo. Le condizioni necessarie per l'ottimalità sono state ricavate per ciascuna strategia e i risultati numerici sono stati presentati. La soluzione ottimale mostra cambiamenti significativi al variare della data di partenza e una procedura e' stata sviluppata per garantire la convergenza utilizzando una sola soluzione di tentativo. Lo stesso problema è stato risolto utilizzando una legge di controllo sub-ottimale in cui gli angoli di spinta rimangono costanti nel sistema di riferimento inerziale durante ognuna degli archi propulsi. É stato condotto uno studio preliminare sugli errori introdotti dalla dispersione di spinta. L'utilizzo di una procedura di ri-ottimizzazione dopo ciascun arco di spinta permette una sostanziale riduzione degli errori nel raggiungimento dell'orbita finale sia per il caso del singolo satellite che nel dispiegamento della formazione. In particolare sono state identificate strategie di dispiegamento intrinsecamente robuste, caratterizzate da un breve arco di spinta finale.

Introduction

Exploration is possible only if new routes are discovered. In space there are infinite routes, but it is not easy to find ones worth to be followed.

Space trajectory design and optimization is the field that studies how to move a spacecraft, subject to different forces, in a three dimensional space in order to accomplish its mission. This field involves many disciplines working together and there are not commercial or academic tools that are suitable for any kind of problem. There are not standards or established working procedures.

Finding a feasible solution is not easy but the most fascinating part in space trajectory design is that, for a given problem, there are multiple trajectories and local optima that fulfill requirements, but difference between a mediocre solution and a good one is sensible. So optimization is a fundamental step.

Improvements in computer science, numerical analysis, propulsion and engineering permit to accomplish complex tasks in a more efficient, economic way or, sometimes, make these tasks feasible.

At present different optimization method are used for trajectory optimization, mainly direct methods, indirect methods, evolutionary algorithms and dynamic programming. The aim of this thesis is to enlarge the application field of the indirect method developed at Politecnico di Torino. Derivation of adjoint variables differential equations was carried on, considering a J8x8 Earth Geopotential model, lunisolar perturbations and solar radiation pressure with Earth conical shadow. The dynamic model has been implemented in a procedure tested on a transfer between HEO orbits.

Highly elliptic orbits are interesting for being a cheap alternative to Halo orbits and they are peculiar from the trajectory design point of view because their high eccentricity breaks the symmetry of perturbations influence.

The main issue was the convergence of the solution, due to the intrinsic sensitivity of indirect methods to the initial tentative guess. A continuation technique was introduced to guarantee convergence using only one tentative guess for all possible departure dates.

The procedure is applied to different boundary conditions and control law. The deployment of two satellites formation has been studied with two different phasing

strategies: Chaser-Target and Cooperative. All the previous problems have been solved also with a control law requiring that the thrust direction is fixed in the inertial frame during each thrust arc.

At the end the errors introduced by thrust dispersion have been analyzed. A re-optimization procedure with an heuristic robust trajectory has been tested in the single satellite case and in the formation deployment, considering different thrust scenarios.

Chapter 1

Indirect method applied to complex problems

Introduction

In this chapter the general problem of satellite deployment will be introduced, considering different scenarios and methods from literature. More details will be given about perturbations and formation flight issues.

The mission Simbol-X will be presented, as case study for indirect methods application.

1.1 Trajectory optimization of satellite deployment

This work is focused on the trajectory optimization, in particular on the application of the indirect method to problem characterized by complex dynamical model where perturbations are present. The optimization method developed is then applied to the deployment of two satellites flying in formation, considering also operational issues such as the re-optimization of the trajectory after the simulation of thrust dispersion errors.

In space trajectory design, the simplest gravitational model used is the two-body problem, where there is a central massive body, that is the source of the gravitational field, and a little one, e.g. is a spacecraft, that does not influence the gravitational field and so it is attracted only by the first body. The only way to modify its trajectory is by using the thrust (generally the only one control). This model is well suited for some conceptual design (i. e. interplanetary trajectories) but it has strong limitations in some scenarios, such as missions around the Earth. In low Earth orbit a big issue is certainly the drag of the highest part of the atmosphere. If the spacecraft is close to the Earth, it is also subjected to the perturbations due to

the non-spherical shape of our planet. When the altitude of the orbit grows, other two actors come on the stage: the Moon and the Sun.

The effects of perturbations are well studied since the beginning of the Space Era: perturbations due the asphericity of the Earth, the presence of Sun and Moon and also effects of solar radiation pressure ([1], [2], [3], [4], [5], [6], [7]). The perturbations are relative small in comparison to Earth's gravity, so the effects can be seen in a mid-long period. Typically perturbations are well studied in station keeping problem, when long operative periods are considered. Analytical and semi-analytical [8], [9] models have been developed to take these perturbations into account, in parallel to numerical methods. These methods were very important in the past when the computational power was small, but also now they are applied successfully in order to speed up computation for long time simulations.

Orbit transfers are shorter in comparison to station keeping time, so perturbation influence is less studied. In most of the geocentric orbit transfers, perturbations are handled using direct methods (MALTO [10], ecc) and, in the last years, dynamic programming (MYSTIC [11]) for trajectory optimization. Another class of methods for trajectory optimization are evolutionary and indirect methods. A deeper analysis, with differences between the methods will be given in chapter 2. Indirect methods are faster and more precise than direct methods, but they may have more convergence issues. Another problem is that indirect methods require the derivation of optimal boundary conditions and derivation of the differential equations for the adjoint variables. They cannot be used as black box solver and they are generally applied to problem with simple dynamics. Application to geocentric problem is less frequent.

Indirect methods are generally used for optimization of impulsive or, at the opposite, very low thrust missions. When these methods are used for geocentric transfers with perturbations, the problem consists in a minimum time optimization in most of the cases and the solution has a continuous thrust. If very low thrust engine is employed, minimum fuel-missions, that consider coast arcs, would be too long. A study on this problem was accomplished by Geffroy and Epenoy [12]. They use an averaging technique to deal with perturbations and a continuation scheme to achieve the optimal solution.

Satellites in geocentric orbit often use chemical thrusters for orbit maneuver. The thrust level is not so high to model the maneuvers as impulsive. At the same time is too high for having a continuous solution. A bang-bang solution is necessary with long coast arcs to keep low the fuel consumption. Several authors (Redding [13], Bertrand [14], Haberkorn [15]) worked on minimum fuel problems with indirect methods, but perturbations were not considered. Thevenet and Epenoy [16] included J2 perturbations in one of their work. They exploited J2 effects to reduce the propellant consumption during the reconfiguration of a four spacecrafts formation; Chuang et al. [17] discuss the effects of atmospheric drag and Earth oblateness for

a fixed-duration transfer.

In "Politecnico di Torino" an indirect method has been used for trajectory optimization for the last two decades and a procedure was developed that mitigates the drawbacks of indirect methods. The formulation of the problem is simplified and so more attention can be paid on strategies to achieve convergence. The procedure has been tested on different problems of interplanetary trajectories [18] [19] [20] [21] [22], but also ascent trajectories of launchers and sounding rockets [23]. The procedure has proven to work with problems involving aerodynamic forces [24] [25].

In the last three years the propulsion group of Politecnico, together with "'Università Sapienza di Roma"', decided to apply the indirect method procedure to a more complex dynamical environment. The research produced different papers on the subject and this thesis collects and puts the work done in a more generic frame.

The introduction of perturbations in the indirect procedure required a new derivation of the adjoint variables differential equations. This was a time consuming task, but derivation was not the greatest issue. The real issue was to understand how perturbations change the optimal solution of the problem and how to get convergence. The last was a big problem considering that indirect methods are very sensible to initial tentative guess and the presence of perturbations makes the problem more sensible.

On the other side, including perturbations enlarges the research field and improves the fidelity of the model; new strategies are sought to avoid the unfavorable perturbations and to exploit the favorable ones. This is useful from a practical point of view but it is also challenging form the intellectual point of view. Highly elliptic orbits are a good testbed for the indirect method procedure applied to perturbative environment. The low perigee is subjected to J2 perturbations and the high apogee is influenced by Luni-Solar perturbations for a large fraction of the revolution period. The procedure can be also used in the future for interplanetary trajectories considering the influences of all the planets, but also for tour design around Jupiter Moons, where there is a big oblateness effect of the giant planet.

From the operational point of view HEO are becoming interesting because they are a cheap alternative to Halo orbits around Lagrangian points for the observations of deep space sky. An example is the concept mission Simbol-X, that is the case study of this thesis. Simbol-X is a mission for observing the sky and the scientific task is accomplished by two satellites working together. The reference orbit of this mission requires the introduction of perturbations but it gives also the chance to deal also with the deployment of two satellites in formation.

Missions can be accomplished by a single satellite or group of satellites. Constellations of satellites work everyday in order to give us telecommunication service, position and surveillance. A constellation is a set of satellites working together for pursuing a specific task/mission. The constellation has to be managed in order to guarantee a certain coverage and the satellites have different orbits. A new paradigm

has been introduced in the last years, that is the satellites in formation flight. In this case satellites work at a closer distance, they have to keep relative distance and velocity in certain ranges and their orbits are very close.

The concept is not new: the Gemini and Apollo capsules had to perform a formation flight before operating a rendez-vous, even if it was only for a short time. Now the idea is to have satellites flying and working in formation, sometimes with very strict constraints.

Some features make more satellites working together an appealing configuration. The formation flight is used by GRACE and GRAIL missions for mapping the gravity of Earth and Moon, by Cluster, Themis and Artemis missions for measuring the interaction of solar wind with the magnetic field of Earth and Moon. Formation flight is also present in proposals, such as Darwin (a telescope for seeking exo-planets), LISA (an interferometer for detecting gravitational waves), SWARM et al. It is possible to say that now there are two types of missions that require formation flight: missions that need a big distance between the satellites in order to have the required accuracy (GRACE, GRAIL and LISA) or missions that have to make measurements over large volumes (CLUSTER, Themi-Artemis).

Sometimes, some of the missions can be accomplished by a single satellite. For example the gravity map performed by GRACE was also performed by GOCE, even if GOCE has a higher space sensitivity, while GRACE has an higher time sensitivity, so the two missions were in part complementary. Other missions, such as LISA, are not possible with a monolithic structure.

Another field of interest represent Cubesats. The new standard of cubesat permits access to space with a relative low cost, but the small dimensions of cubesats (even in the composite structure of three modules) do not permit to have complex system on a single spacecraft. A formation of cubesats could accomplish more complex tasks and have some fault tolerant formation design. They can be used also coupled with bigger spacecrafts. Another possible future application is the formation flight needed to auto-assembly the next generation Space Station or Deep Space Habitat.

Formation flight is a very prolific field of studies, considering free or tethered satellites in formation, but often the studies are focused on the control law and the stability of the formation. Relative few studies are oriented to deal with the deployment of the formation, even if the maneuver can be tricky, in particular when perturbations are present.

The classical deployment strategy is the chaser-target, where a satellite (the target) applies its own optimal strategy, while the other one (the chaser) reaches the orbit of the first one. In this thesis the chaser-target approach has been studied together with the cooperative approach. Cooperative deployment strategy means that the two satellites perform the transfer optimizing the overall final mass and not only the target final mass. The sum of the masses of the two satellites in cooperative

strategy is larger than the same value in chaser-target strategy, while target final mass will be lower and chaser one higher.

At the end of the thesis some operative studies have been done about the application of indirect method to more operational problem, such as consider thrust laws more simple to be realized than the optimal control law.

The last topic of this thesis is the study of the influence of thrust dispersion errors in the fulfillment of mission requirements. A simulation of the errors in direction and magnitude of the thrust vector was performed and the final errors on the boundary constraints were considered. An open loop control is not suitable, even if only thrust errors are considered (not considering orbit determination errors). So re-optimization close loop was used and sub-optimal robust solutions were seek.

1.2 Case study: Simbol-X

The indirect optimization procedure with perturbations can be applied to different case studies and different configurations. The case study of this thesis is the mission concept Simbol-X, a French-Italian mission (now canceled) for the observation of the sky in the hard X-ray.

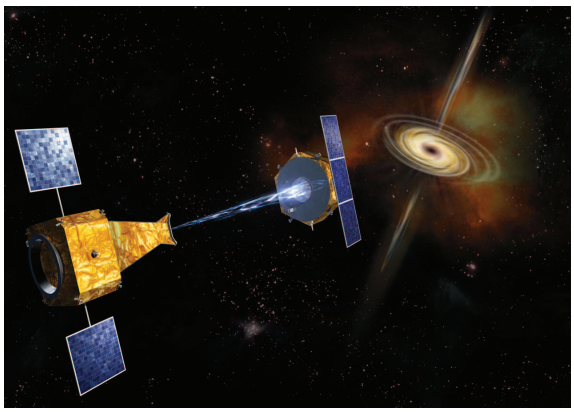

Figure 1.1: Artistic Impression of Simbol-X. Credit: CNES

In 2001 CNES, the French Space Agency, wanted to build a formation flying demonstrator. The French and Italian scientific community proposed a mission for observing the universe in the hard X-ray range. In the past other missions explored the X-ray with lower energy ($< 10\,\mathrm{KeV}$): UHURV, Ariel-V, HEA01, Einstein, ROSAT, Chandra, XMM-Newton. These missions permitted to discover X-ray bursts in the galaxy.

Other missions were launched for the observation of hard X-rays (BeppoSAX, INTEGRAL), but the sensitivity and angular resolution was low with respect to

X-ray telescopes and so it is hard to individuate hard X-ray sources. These sources are important to study the accretion physics in black holes and particle acceleration mechanism. The idea was to bring the X-ray mirror technology to the observations of hard X-rays, but this feature requires long focal lengths.

In order to reach the scientific requirements for observation, the focal length should be between 20 m and 30 m. It is not possible to have this instrument in a monolithic structure, so the telescope has the mirror and the detector on two different satellites flying in formation.

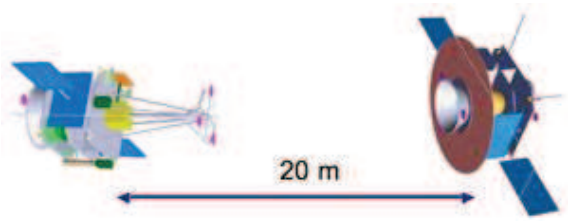

Figure 1.2: Distance between satellite: the left satellite is the detector and the satellite on the right is the mirror. Credit: CNES

The mission should operate for at least 2 years with a chance to be extended. The telescope points the target and has to perform a long observation (100 ks or more) on the same target. In order to have stable images the two satellites have to keep the focal length with an error ±10 cm. The scientific requirements give constraints to the choice of the orbit. The observation can be done only above 73000 km, in order to avoid disturbances form Van Allen belt. At the beginning, the orbit chosen was an halo orbit around L2 Sun-Earth Lagrangian point, but then the idea was to use a cheaper geocentric elliptic orbit.

Gamet et al. [26], [27], Fontedecaba [1] describe the mission overview, the constraints and the problem related with formation keeping and orbit raising. The main constraint for the choice of the operative orbit are: the observation constraints; the launcher mass capacity; propellant mass budget for orbit maneuver, formation keeping, pointing and end-of-life maneuver; link budget.

The constraint of staying above the Van Allen belt requires high semi-major axis. At the beginning a 7 sidereal-days (90% of observation time) orbit was chosen, but it was not compatible with link and mass budget and so a 4 days orbit (83% of observation time) was selected. The selected launcher was a Soyouz with a Fregat upper stage. The launcher capacity for the chosen transfer orbit is around 2300 kg. The choice of the value of the perigee is linked to three factors. The first is that the hydrazine budget for formation keeping increases when the perigee altidtude is low (5000 km altitude). Possible values were in the range 15000-20000 km of altitude. On the other side a higher altitude of perigee requires higher propellant budget for

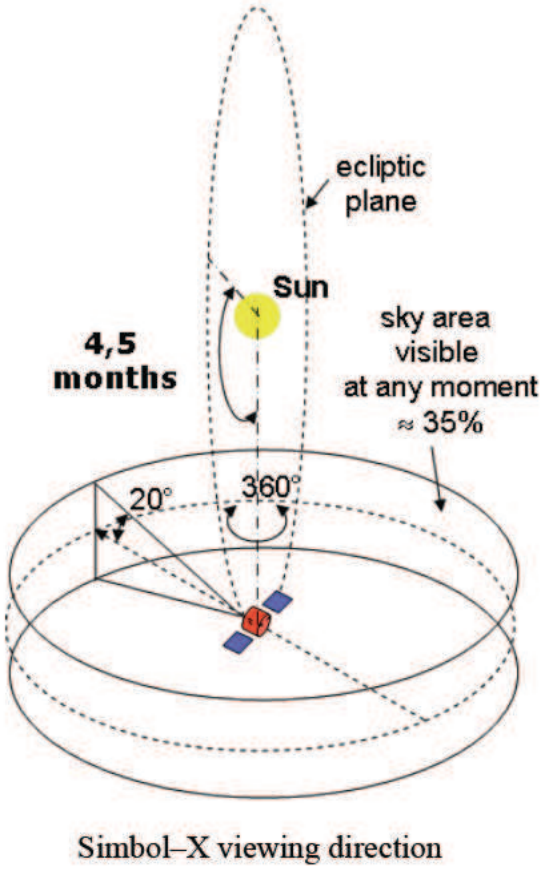

Figure 1.3: Viewing direction. Credit: CNES

perigee raising. In order to improve also the link budget, the lowest value of the perigee was chosen.

The mission starts with the launch, then the perigee raising is performed. This maneuver is strongly influenced by the position of the Moon that may make the two satellites plunging in the atmosphere. On the other side, if a good departure date is chosen, the Moon may stay in a favorable position and help increasing spacecraft perigee. In this phase the two satellites are controlled independently from the ground in the so called free formation flying. When the two satellites are close enough (10 - 30 km) a radio frequency sensor establish an inter satellite link. In this phase the satellites maneuver are still computed on the ground, but avoidance maneuvers are computed on board. In the formation acquisition mode the formation is controlled by on board Guidance, Navigation and Control subsystem.

In the coarse formation mode the distance between satellites is reduced to 20 m.

In the fine formation mode the formation is controlled by optical sensors and cold gas thrusters: this is the scientific mode.

The work of this thesis is focused on the application of the indirect method to the delivery phase/perigee raising. The aim is to apply the indirect method to this complex problem, to study the influence of the perturbations on the optimal solution either in terms of performance index or in terms of optimal strategy.

Conclusions

In this chapter the problem of satellite deployment was presented. After the review of existing literature, it has been proposed to apply the indirect method developed at "Politecnico di Torino" to more complex problems, involving Earth oblatness, Moon and Sun perturbations. The deployment of two-satellite formation in HEO was considered a good testbed due to the complexity of the involved dynamic and, at the same time, for the increasing interest of the scientific community in the exploitation of HEO as cheaper alternative to Halo orbits and in the appealing formation flight features. The mission Simbol-X proposal was presented as case study.

Chapter 2

Methods for trajectory optimization

Introduction

The general statement of an optimization problem will be introduced in this chapter. After a brief survey of direct and evolutionary methods, a deeper description of the indirect method used in this thesis will be given.

2.1 Optimization problem: definition and taxonomy

The work presented in this thesis concerns the transfer trajectories of a two-satellites formation, with the Earth as central body. The dynamic environment is complex, described by non linear equations. Every little perturbation can change the final orbit, so the design is challenging and the optimization process is necessary in order to have a feasible mission. When finite thrust is used the optimization is even more difficult so the optimization method becomes important.

In Politecnico di Torino prof. Bussi established an optimization research team for solving problem linked with propulsion and trajectory mission design. In this team an indirect method was developed and applied to different problems: interplanetary mission, such as Earth-Mars transfers or travel to asteroid, deviation of asteroid with kinetic impact, launcher ascent optimization and sounding rocket flight. In the last years an hybrid evolutionary algorithm was developed in the team, for solving problems such as impulsive transfers and other applications. The direct method has not been used in the Politecnico team, but there was a first tentative of a direct method coupled with the indirect method. The research of the last three years was

focused on the use of the indirect method in a perturbed environment and also with more than one spacecraft in formation.

It is important to describe the optimization tool used for the problem studied in this thesis, but it can be useful in the this chapter a brief survey of other optimization methods. The material is taken form the notes of prof. Casalino lessons, Repetto's course in Politecnico di Torino [28], Stanford [29] and Princeton course [30] and the paper of Betts about the survey of the optimization methods [31]. More detailed information can be found in these resources.

Most of the theoretical bases have their roots in the middle of twenty th century, but the implementation of these methods was difficult because the low computational power available. So it is possible to see a parallel path in which optimization methods improve their performances and number of applications side by side the improvements in computational power. An optimization method can be used in different applications, but not all methods are good for each one. Changing the field of application or also, in the same field, the type of the problem, can require a tuning of the algorithm.

The aim of the optimization is to maximize or minimize an objective function. This is called single objective optimization and it is the same carried out in this thesis.

There is also the multi-objective optimization where there are multiple performance index. Citing the definition of Osyczka (1985), multi-objective optimization find a vector of decision variables and optimizes a vector function whose elements represent the objective functions. The performance index are usually in conflict, so the optimization process aims to find acceptable values of the objective functions, following some criteria useful to the user. Generally the aim is to find a trade-off between them.

There are different ways to deal with multi-objective optimization: the most common are the use of a Pareto front or summing all the performance indexes in a single one.

For the first one the meaning of dominance is involved. The Pareto front is a set of solutions, each one is not dominated by other solutions. The problem becomes highly computational demanding. Another way is to have a single performance index that is the linear combination of the objective functions. The sum of all the indexes requires the choice of weights and the optimal solution strongly depends on this choice. Changing the weights is equivalent to move on the Pareto front.

Another taxonomy is about global/local optimization. Local optimizers start from a tentative solution and find a local minimum (maximum) which depends on the convergence radius of the method. A global optimizer virtually explores all the solution space and it is able to find the global optimum.

In general, an optimization problem can be static or dynamic, requiring different types of methods. Trajectory is the set of the different positions of the spacecraft

during time, so it is a dynamical problem and the independent variable is the time t. Sometimes it can be convenient to change the independent variable. The trajectory can be split in different phases or arcs, each one from t_{j-1} to t_j. The different phases are useful for using different constraints, different state equations or also for considering a multi-branch trajectory.

In the most general case the trajectory is described by the state variables $\boldsymbol{x}(t)$ and the control vector $\boldsymbol{u}(t)$. It is also possible to have static parameters that are collected in vector $\boldsymbol{c}$. The dynamic system behavior is nonlinear and that makes the optimization process more difficult than a static problem, but the time dependence builds a structure in the solution, because all the state variables have to be continuous inside a phase, while they can be discontinuous between two phases.

The system is defined by a set of explicit differential equation, even if it should also be implicit. Usually

$$\frac{\mathrm{d}\boldsymbol{x}}{\mathrm{d}t} = \boldsymbol{f}(\boldsymbol{x}(t),\boldsymbol{u}(t),\boldsymbol{c},t) \tag{2.1}$$

Splitting the trajectory in phases allows to have different dynamic equation for each arc (i.e. different Thrust level, different engine). As said before, each phase is identified by an initial and a final time.

The set of boundary conditions can be indicated as:

$$\boldsymbol{\psi}_{j-1_l} \leq \boldsymbol{\psi}(\boldsymbol{x}_{(j-1)_+},\boldsymbol{x}_{j_-},\boldsymbol{u}_{(j-1)_+},\boldsymbol{u}_{j_-},\boldsymbol{c},t_{(j-1)_+},t_{j_-}) \leq \boldsymbol{\psi}_{j-1_u} \qquad j = 1,\ldots,f \tag{2.2}$$

where j is the phase number, t_0 is the initial point and t_f the final one. The subscripts l and u indicate respectively lower bound and upper one. All the interior point are called junction points, where two or more phases (if the trajectory is multi-branch) are linked. The boundary conditions are in general inequality constraints, but they can consider also equality ones. The boundary conditions can be complex functions, but also simple linear constraints on the state variables or on the controls.

The solution can also fulfill algebraic path constraint in the form

$$\boldsymbol{g}_{p_l} \leq \boldsymbol{g}_p(\boldsymbol{x},\boldsymbol{u},\boldsymbol{c},t) \leq \boldsymbol{g}_{p_u} \qquad j = 1,\ldots,f \tag{2.3}$$

In the next paragraphs, if no specified, $\boldsymbol{x}$ and $\boldsymbol{u}$ stand respectively for $\boldsymbol{x}(t)$ and $\boldsymbol{u}(t)$. In some case also the quadrature

$$\int_{t_0}^{t_f} \boldsymbol{q}[\boldsymbol{x},\boldsymbol{u},\boldsymbol{c},t]\mathrm{dt} \tag{2.4}$$

case can be evaluated. The quadrature, together with the differential equation (2.1) and the path constraint (2.3), are referred as the continuous functions inside

each phase. The boundary conditions, that can be also linear, are referred as the point functions.

The objective functions can be continuous or discrete. For the trajectory optimization problem, generally the assumption is that the objective function is continuous and differentiable with respect to the variables.

In the Mayer formulation the performance index J is written as

$$J = \phi(\boldsymbol{x}_0,\boldsymbol{x}_{1\pm},...,\boldsymbol{x}_f,t_0,t_{1\pm},...,t_f,\boldsymbol{c}) \tag{2.5}$$

Another formulation is the Lagrangian one

$$J = \sum_{j=i}^{f} \int_{t_{(j-1)+}}^{t_{(j)-}} \Phi(\boldsymbol{x},\dot{\boldsymbol{x}},t)\mathrm{dt} \tag{2.6}$$

If the J is the sum of the integral of the Lagrangian formulation and the scalar of the Mayer formulation, it is called the Bolza problem. It is always possible to pass from one formulation to the other one with the help of auxiliary variables.

Now it is possible to define the optimization problem: find the control $\boldsymbol{u}$ and parameters vector $\boldsymbol{c}$ to minimize (or maximize) the performance index J, respecting the boundary conditions. The search of the optimal solution can be performed using only the objective function evaluation (as in the evolutionary methods), the gradient evaluation or also the Hessian evaluation. Sometimes the taxonomy is not so neat. For example the Newton method, the most used in trajectory optimization, uses the computation of the Hessian, while the Quasi-Newton Method approximates the Hessian using only the evaluation of the gradient. In the optimization a feedback control law can be used, such as the Q-law function introduced by Petropoulos et al. [32]. In the present thesis a feed-back is used to mitigate the error introduced by possible dispersions in a real mission, but in this case it is not involved in the optimization process.

In the next paragraphs three methods will be presented: direct methods, evolutionary methods and the indirect method used in this work. Other methods for the optimization can be used, such as the dynamic programming or the differential dynamic programming, that mitigates the curse of dimensionality of its predecessor. It is worth to say that dynamic programming, even if it has not a large field of application, is very important from the theoretical point of view.

2.2 Direct Algorithms

Direct algorithms are very common in the field of trajectory optimization. Both direct and indirect methods make use of NLP (Non Linear Programming) for the search of the optimal variables, but the main difference is that direct methods have

a direct evaluation of the performance index and the constraints of the problem. The indirect methods only consider the constraints of the problem and optimality conditions. The main source for this paragraph is the paper of Betts about numerical methods for Trajectory Optimization.

There are different applications of direct methods, but one of the most useful is the direct transcription that works with discrete system. It can be applied without deriving optimality conditions and does not require an a priori definition of phase sequence when path inequalities are present. The time domain is divided into intervals, defining a grid

$$t_0 < t_i < \ldots < t_M = t_f \tag{2.7}$$

The problem variables to be optimized are the state and control variables at the grid points:

$$\boldsymbol{x} = \{\boldsymbol{y}_0,\boldsymbol{u}_0,\boldsymbol{y}_1,\boldsymbol{u}_1,\ldots,\boldsymbol{y}_M,\boldsymbol{u}_M\} \tag{2.8}$$

The aim is to maximize the performance index $\phi(\boldsymbol{x})$. ϕ is a maximum if $\mathrm{d}\phi \leq 0$ for any choice of $\mathrm{d}\boldsymbol{x}$. For small variations it is possible to adopt a second order Taylor's expansion of ϕ.

$$\phi(\boldsymbol{x} + \mathrm{d}\boldsymbol{x}) = \phi(\boldsymbol{x}) + \boldsymbol{g}^{\mathrm{T}}\mathrm{d}\boldsymbol{x} + \frac{1}{2}\mathrm{d}\boldsymbol{x}^{\mathrm{T}}\boldsymbol{H}\mathrm{d}\boldsymbol{x} \tag{2.9}$$

where $\boldsymbol{g}$ is the gradient defined as

$$\boldsymbol{g} = \frac{\partial\phi}{\partial\boldsymbol{x}}^{T} = \nabla_{\boldsymbol{x}}\phi = \begin{bmatrix} \frac{\partial\phi}{\partial x_1} \\ \frac{\partial\phi}{\partial x_2} \\ \vdots \\ \frac{\partial\phi}{\partial x_n} \end{bmatrix} \tag{2.10}$$

while $\boldsymbol{H}$ is the Hessian, the nxn symmetric matrix

$$[\boldsymbol{H}] = \frac{\partial\left(\frac{\partial\phi}{\partial\boldsymbol{x}}\right)^{T}}{\partial\boldsymbol{x}} = \frac{\partial\boldsymbol{g}}{\partial\boldsymbol{x}} = \begin{bmatrix} \frac{\partial^2\phi}{\partial x_1\partial x_1} & \frac{\partial^2\phi}{\partial x_2\partial x_1} & \cdots & \frac{\partial^2\phi}{\partial x_n\partial x_1} \\ \frac{\partial^2\phi}{\partial x_1\partial x_2} & \frac{\partial^2\phi}{\partial x_2\partial x_2} & \cdots & \frac{\partial^2\phi}{\partial x_n\partial x_2} \\ & \vdots & \ddots & \\ \frac{\partial^2\phi}{\partial x_1\partial x_n} & \frac{\partial^2\phi}{\partial x_2\partial x_n} & \cdots & \frac{\partial^2\phi}{\partial x_n\partial x_n} \end{bmatrix} \tag{2.11}$$

For an unconstrained optimization, the necessary condition for ϕ to be a maximum (or a minimum) is that the gradient $\boldsymbol{g}$ is zero. To identify the nature of the stationary point, the second variation of ϕ (the Hessian) has to be analyzed. For a maximum, $\mathrm{d}\boldsymbol{x}^{\mathrm{T}}\boldsymbol{H}\mathrm{d}\boldsymbol{x} \leq 0$ is required for any $\mathrm{d}\boldsymbol{x}$, that is $\boldsymbol{H}$ negative semidefinite for a maximum (non-positive eigenvalues). For a minimum the eigenvalues have to be non-negative. The sufficient conditions to have a maximum is that $\boldsymbol{g} = 0$ and

$\mathrm{d}\boldsymbol{x}^{\mathrm{T}}\boldsymbol{H}\mathrm{d}\boldsymbol{x} < 0$ for any $\mathrm{d}\boldsymbol{x} \neq 0$, that is $\boldsymbol{H}$ negative definite for a maximum (negative eigenvalues).

The aim of the optimization is to have $\boldsymbol{g}(\boldsymbol{x}) = 0$, that is true for a root $\boldsymbol{x}^*$. The basis for the root finding is Newton's Method, that here is explained in brief. This method is iterative and starts from a tentative guess $\boldsymbol{x}^0$, where the superscript is no an exponent, but the number of the iteration. If a generic $\boldsymbol{x}^r$ estimation at the r^{-th} iteration is considered, the new estimation is:

$$\boldsymbol{x}^{r+1} = \boldsymbol{x}^r + K_1\boldsymbol{r} \tag{2.12}$$

where K_1 is called the scalar step length and $\boldsymbol{r}$ is the search direction. In literature the search direction is sometimes indicated as $\boldsymbol{p}$, but the other notation is preferred to avoid confusion with other symbols.

The search direction $\boldsymbol{r}$ is computed using the Hessian:

$$\boldsymbol{H}(\boldsymbol{x})\boldsymbol{r} = -\boldsymbol{g}(\boldsymbol{x}) \tag{2.13}$$

The root-finding method can be generalized using different matrices for computing the search direction. In general, the matrix used has to be non-singular (in other words invertible). An issue of this method is that the initial estimation has to be close to the root $\boldsymbol{x}^*$, otherwise the method may diverge. In order to stabilize the method the K_1 step length can be reduced. This procedure is called a line search. In general what is done by this procedure is to find a value of K_1 so that a function called merit function is lower than the previous iteration. One possible choice is the gradient

$$\left\|\boldsymbol{g}(\boldsymbol{x}^{r+1})\right\| \leq \|\boldsymbol{g}(\boldsymbol{x}^r)\| \tag{2.14}$$

This is a common choice for indirect methods. For direct methods generally the performance index is chosen as merit function

$$\left\|\phi(\boldsymbol{x}^{r+1})\right\| \leq \|\phi(\boldsymbol{x}^r)\| \tag{2.15}$$

When this merit function is used it may happen that the search direction points uphill instead of downhill, and so the search direction has to be recomputed. In other words, if the function ϕ were a bi-dimensional convex function, it would be like a bowl. With the second order Taylor's expansion the Newton Method is able to find the bottom of the bowl, that is where $\boldsymbol{g}(\boldsymbol{x}) = 0$. The function is convex and the minimum is only one (specular situation is for a concave function where there is only one maximum). Generally speaking the function ϕ is not convex (o concave) and it has multiple local minimum and maximum and so different peaks and valleys. The Newton method, starting from a first guess, approximate the neighborhood of the estimation $\boldsymbol{x}$ as a bowl to find the search direction to the bottom of the approximated

bowl. But the real shape of the function is different from a bowl, so following the search direction it is possible to have a value of ϕ higher than in the previous step or a gradient higher than in the previous step. Indirect methods, commonly but not always use the gradient as the merit function, so they may be entrapped in a local minimum. Direct methods generally have a bigger convergence basin because they use the performance index as merit function.

The optimization problem becomes more complex when constraints are involved. For the sake of simplicity here only the equality constraints $\boldsymbol{\psi}(\boldsymbol{x}) = 0$ are considered. If $\boldsymbol{x}$ is a n-component vector and $\boldsymbol{\psi}$ is a m-component vector, it has to be $m < n$. The feasible points are those which satisfy the relationship $\boldsymbol{\psi}(\boldsymbol{x}) = 0$. The choice $\mathrm{d}\boldsymbol{x}$ is said admissible if it verifies $\boldsymbol{\psi}(\boldsymbol{x} + \mathrm{d}\boldsymbol{x}) = 0$.

At a feasible point, ϕ is a maximum if $\mathrm{d}\phi \leq 0$ for any admissible choice of $\mathrm{d}\boldsymbol{x}$. Any admissible variations require $\mathrm{d}\boldsymbol{\psi} = \boldsymbol{\psi}(\boldsymbol{x} + \mathrm{d}\boldsymbol{x}) - \boldsymbol{\psi}(\boldsymbol{x}) \leq 0$. There are different ways to maximize the function ϕ considering also the constraints. One of the possibilities is to optimize the augmented function

$$\phi^* = \phi(\boldsymbol{x}) + \boldsymbol{\lambda}^T \boldsymbol{\psi} \tag{2.16}$$

where $\boldsymbol{\lambda}$ is a m-component vector of adjoint parameters to be determined. ϕ and ϕ^* have the same value if the constraints are satisfied. In literature, the expression

$$L(\boldsymbol{x},\boldsymbol{\lambda}) = \phi(\boldsymbol{x}) - \boldsymbol{\lambda}^T \boldsymbol{\psi} \tag{2.17}$$

can be found. This is the Lagrangian and it is equivalent to Hamiltonian H, except for the minus sign before the $\boldsymbol{\lambda}$ vector. The second-order Taylor's expansion of the augmented function ϕ^* is

$$\phi^*(\boldsymbol{x} + \mathrm{d}\boldsymbol{x}) = \phi^*(\boldsymbol{x}) + (\boldsymbol{g}^{\mathrm{T}} + \boldsymbol{\lambda}^{\mathrm{T}} [\boldsymbol{G}])\mathrm{d}\boldsymbol{x} + \frac{1}{2}\mathrm{d}\boldsymbol{x}^{\mathrm{T}} [\boldsymbol{H}^*] \, \mathrm{d}\boldsymbol{x} \tag{2.18}$$

where $\boldsymbol{g}$ is the gradient as usual, $[\boldsymbol{G}]$ is the Jacobian and $[\boldsymbol{H}^*]$ is the augmented Hessian. The Jacobian is the first order expansion of the constraints

$$[\boldsymbol{G}] = \left[\frac{\partial \boldsymbol{\psi}}{\partial \boldsymbol{x}}\right] = \begin{bmatrix} \frac{\partial \psi_1}{\partial x_1} & \frac{\partial \psi_1}{\partial x_2} & \cdots & \frac{\partial \psi_1}{\partial x_n} \\ \frac{\partial \psi_1}{\partial x_2} & \frac{\partial \psi_2}{\partial x_2} & \cdots & \frac{\partial \psi_2}{\partial x_n} \\ & \vdots & \ddots & \\ \frac{\partial \psi_m}{\partial x_1} & \frac{\partial \psi_m}{\partial x_2} & \cdots & \frac{\partial \psi_m}{\partial x_n} \end{bmatrix} \tag{2.19}$$

and the augmented Hessian is

$$[\boldsymbol{H}^*] = [\boldsymbol{H}] + \frac{\partial \left[\left(\frac{\partial \boldsymbol{\lambda}^T \boldsymbol{\psi}}{\partial \boldsymbol{x}} \right)^T \right]}{\partial \boldsymbol{x}} \tag{2.20}$$

The component of the augmented Hessian is expressed as

$$H^*_{ij} = H_{ij} + \sum_{k=1}^{m} \lambda_k \frac{\partial^2 \psi_k}{\partial x_i \partial x_j} \tag{2.21}$$

The first-order necessary condition for the augmented function is

$$\boldsymbol{g} + [\boldsymbol{G}]^T \boldsymbol{\lambda} = 0 \tag{2.22}$$

which gives n scalar conditions. With the m conditions $\boldsymbol{\psi} = 0$ there are $n + m$ equations for finding $\boldsymbol{x}$ and $\boldsymbol{\lambda}$. Eq. (2.22) build a relationship between the gradient of the function ϕ and the gradient of the constraints. The linear system to compute the search direction is called Kuhn-Tucker (KT) or Karush-Kuhn-Tucker system and it is equivalent to the minimization of the quadratic form

$$\frac{1}{2}\boldsymbol{r}^T \boldsymbol{H}^* \boldsymbol{r} + \boldsymbol{g}^T \boldsymbol{r} \tag{2.23}$$

with the constraints

$$\boldsymbol{G}\boldsymbol{r} = -\boldsymbol{\psi} \tag{2.24}$$

This is called Quadratic programming.

When inequalities are considered, the problem is to define which constraints are active, and so they have to be treated as equality constraints, and which ones are inactive, and so they are not considered in the optimization. A very common method to handle the inequality constraints in the realm of space trajectories optimization is the sequential quadratic programming (SQP).

All the techniques described until now are optimization methods and they are applied to the trajectory optimization. The trajectory problem can be stated in different way.

One possible choice is direct shooting. In this case the unknowns of the problem are the initial state variables, the initial time, the parameters and the parameters of the control $\boldsymbol{u}$. The initial values are propagated until the final time t_f is reached, and the output of the problem is the value of the function ϕ and the constraints $\boldsymbol{\psi}$. One of the issue of this method is that the problem is very sensitive to the initial values that are propagated along the whole trajectory.

To avoid that small changes introduced at the beginning of the trajectory can propagate into large changes at the end, the trajectory is broken into shorter segments. The initial values of the dynamic variables at the beginning of each segment are the new unknowns. New constraints are present to join all the segments. The number of unknowns grows with the number of segments, but the Jacobian is sparse because the segments are uncoupled. The multiple shooting improves robustness of

the method, but increases the number of unknowns and constraints. It needs also to define constrained and unconstrained subarcs a priori.

Another direct method is the transcription or collocation method. The time domain is broken in smaller intervals and each point is called grid point. The unknowns are the state and control variables at the grid points and their parameters, such as initial and final time. The initial differential equation are substituted by defect constraints, that are the errors at arc junctions after the integration of one step. The non linear programming problem is large, but the matrices are sparse. This method is versatile and robust and does not require to establish inequality path constraints a priori.

2.3 Evolutionary Algorithms

A class of Algorithms that is widely used nowadays are the Evolutionary Algorithms. They are global optimizer in the sense that they can potentially find the global optimum of the problem. Direct and Indirect methods strongly depend on the initial solution, even if in different ways. Evolutionary methods take inspiration from the natural life and sometimes they are addressed also as biomimetics. Evolutionary algorithms are good for testing biological or social theories, but they are also good for optimizing. Every solution is considered as an individual and new solutions are generated in different ways.

Three features are fundamental in the evolutionary algorithms: the new solutions are obtained by little changes and some features have to be inherited from the old individuals; there is a selection of the individuals; the fittest individuals survive and transmit their features to the new individuals. In nature the fittest individual is the one who survives, but in an optimization process the performance index is the measure of the fitness and is linked in some way to the fitness function. The fitness function can be fixed or mutable and it is called also fitness landscape. Generally there is a parent population of individuals that generates an offspring generation. In this process the parents are chosen with a bias towards the higher fitness.

There are a lot of different algorithms that belong to this class, some are quite equivalent and each one can have different variants. These algorithms do not make any general assumption about fitness landscape, so they are pretty versatile. They have a stochastic behavior so they are also intrinsically robust. They can handle also multi-objective function and they generally give a set of possible solutions and it is task of the user chooses the suitable one.

Some issues are obviously present. Having no assumptions about the fitness landscape, the parameters space has to be searched in a "blind way", so more parameters are present, more function evaluations are necessary. In complex problem, where many parameters are present, the use of those algorithms is limited by

computer-time, in comparison with problem of the same complexity treated by direct or indirect methods. A common practice is to use an approximate model with an evolutionary algorithm and then using the solution as a tentative guess for an other optimizer with a more complex model.

Another issue is that different algorithms behave in different ways with different problem. Generally an algorithm can be evaluated considering its speed of convergence, efficiency and accuracy. One single algorithm is generally very strong in one feature and average on the other two for a certain problem.

A hybrid optimization method, which runs GA, DE, and PSO in parallel, was in the past developed at Politecnico di Torino. The characteristics of the algorithms and their synergistic use have been discussed in detail [33–35] and only the main features are described here. In the last version an initial diversification phase based on enhanced continuous tabu search is introduced into the algorithm with the aim of improving the algorithm performance (namely, probability of finding the global optimum) and possibly reducing the required number of function evaluations to attain the optimum.

2.3.1 Genetic Algorithm

GA are the most common evolutionary algorithms, introduced by John Holland [36]. They are based on the observation of natural evolution. Each individual is a string written with a certain alphabet. The string plays the role of a chromosome and encodes the individual. The genotype is the set of chromosome value that is uniquely mapped onto the decision variable (phenotype). So the string is decoded into its phenotypic values. A phenotype can correspond to different genotypes. The chromosome can be expressed in binary string, but in the realm of trajectory optimization a real-code formulation is usually adopted and each individual is characterized by the real values of the optimization variables. Each individual has a fitness function depending on the value of the performance index and individuals with higher fitness have a higher probability of being selected for mating with other individuals. This is the principle of survival of the fittest and it is used to have better and better approximations of the optimal solution. The initial population is created randomly and for each generation parent individuals are selected. In the code used in Politecnico they are chosen by means of tournament selection. Deb's crossover [37] is used to create children solutions which replace the old individuals in the new generation. Elitism is used to avoid the loss of good individuals caused by other genetic operators. Mutation is applied to the new population to increase the number of explored solutions and keep diversity in the population. Some of the variables are changed, according to a small specified probability. The objective function of each individual of the new generation is finally evaluated; the worst ones are discarded and replaced by the elite individuals of the former generation. The whole procedure

is repeated for a fixed number of generations or until a prefixed number of function evaluations is reached. GA algorithms permit to explore a population of points in parallel, while the direct and indirect method explore the neighboring of a single point at one time. GAs do not require derivative computation or other auxiliary information. They use probabilistic rules, not deterministic ones, so can give different results in different runs. GA provide a set of potential solution, but the final solution is generally chosen by the user. Their probabilistic nature can be utilized for a robust optimization.

2.3.2 Differential Evolution

DE [38, 39] is similar to GAs. There are parents and offspring and the selection is made considering the fitness function, but the selection/crossover mechanism is different. For the generation offspring, four individuals (the minimum size of population) are chosen randomly. New vectors of variables are generated by adding the weighted difference between the two vectors to a third one. The resulting individual is compared to a predetermined population member. If the fitness function of the new individual is higher, it replaces the one it was compared to; otherwise, the old individual is retained. There are a lot of variation of this simple method and the value of the amplification of the difference vector can change depending on the problem.

2.3.3 Particle Swarm Optimization

PSO [40] [41] [42] [43] [44] is a social optimization algorithm. It is based on the interaction of simple individuals with the environment and between each other. Another algorithm belonging to the category of social optimization is the Ant Colony Optimization ACO. The PSO is inspired by social behavior of bird flocking or fish schooling. The collective behavior of the individuals shows an emerging intelligence that is called swarm intelligence. In this algorithm the current population moves across the search space, while in GA and DE there is the generation of new individuals. The individual is called particle and it has a position (that are the parameters of the problem) and a velocity vector, which rules the motion of the particle. The particles move through the domain and each particle updates its instantaneous velocity at each iteration in order to improve the solution. The velocity is changed to move the particle toward the best solution that the particle itself has reached in the previous iterations (cognitive acceleration) and toward the best solution that any particle in the population has reached (social acceleration). So the PSO algorithm has memory. In GA and DE all the individuals share information with all the population, while in PSO only the Best individual gives information to the group. For this reason the PSO algorithm converges very quickly.

2.3.4 Ant Colony Optimization

Ant Colony Optimization [45] [46] is another bio-inspired algorithm and it belongs to the category of social optimization. It takes inspiration from the behavior of ants that have limited cognitive faculties as individuals. Ants usually communicate with the colony using pheromones, that are applied to the ground. The pheromone has limited lifetime before evaporating. The ants explore the nest neighborhoods with an initial random walk, but when food is found, the ant comes back to the nest leaving pheromones on the ground. The other ants, at each step, can decide to explore the neighborhoods or to be greedy and follow the path with the higher pheromone concentration. The shortest path between the nest and the food has the higher quantity of pheromones because they have less time for evaporating, so ants follow the shortest path with an higher probability.

There are many different implementations of ACO and they are used for combinatorial problem, minimum walk in a graph, etc.

2.3.5 Branch and Bound

First proposed by Land and Doig [47], the branch and bound (and prune) method is used for integer and discrete optimization. There is also an implementation that use the the cutting plane algorithm. The procedure is based on three step: branching, bounding and pruning. The aim is to optimize (i.e. minimize) the function $\phi(\boldsymbol{x})$ in a set $\boldsymbol{S}$ of candidate solution of integer or discrete decision variables. The first step is recursive generation of subset S_i (branching). This operation build a tree, that is a set of nodes connected by edges. The function $\phi(\boldsymbol{x})$ has a minimum value v_i in the subset S_i and the upper and lower bounds for the minimum value of $\phi(\boldsymbol{x})$ are computed (bounding).

If the lower bound for some tree node is greater than the upper bound of another node (in minimization case), this maybe safely discarded (pruning). The entire procedure stops when S is a single element or if the upper bound matches the lower bound.

2.3.6 Simulated Annealing

Simulation annealing [48] takes inspiration from annealing in metallurgy, a technique that involves heating and cooling in order to increase crystal size dimension. The main idea is to have an algorithm exploring neighboring solutions with a decreasing probability of accepting worse solution

The procedure starts from a state s and can decide to move in other state or remain in the same state. The decision is probabilistic, in order to have the possibility to fully explore the solution space. The aim is to minimize the energy, that

can be the performance index.

The acceptance probability function $P(e,e',T)$ defines the probability to move in another state and it depends on the energy of the present state e, the energy of the neighboring state e' and the time-varying parameter, the temperature T. The probability has to be positive (but small) if $e' > e$. When T decreases the algorithm has to become more greed and to "prefer" down-hill moves.

2.3.7 Cooperative hybrid algorithm

An evolutionary algorithm can be evaluated considering the speed of convergence, the efficiency and the accuracy, but these performance strongly depends on the nature of the problem. A specific algorithm can have very good speed of convergence, but be average in the other performance.

The use of an hybrid algorithm, where different programs work sinergistically, can improve the overall performance. The different algorithms can exchange information using migration or clonation of the best individuals. The different populations can work on different domains, using the island model.

At Politecnico di Torino a similar algorithm has been developed (*Hemoglop: Hybrid Evolutionary Multi-Optimisers Global Optimisation Tool*) and GA, PSO and DE are used. In order to have a good exploration of the solution space, the search of the optimal one can start with a TS based diversification phase. Tabu search is an algorithm originally developed by Glover [49, 50], which has been successfully applied to a variety of combinatorial optimization problems. The parameters for trajectory optimization are continuous, so it is more suitable an adaptation of TS to continuous optimization problems, called enhanced continuous tabu search [51], which is inspired by Glover's approach.

A number of random solutions depending on the number of variables are initially produced; the diversification phase starts from the best solution s among these. A set of a limited number of new solutions is generated during each iteration, dividing the domain in hypercubes, which surround the current solution s. A new solution is picked randomly in every subdomain. A tabu list, which contains solutions belonging to regions of the search domain that have already been explored, is created to avoid the risk of the appearance of a cyclic behavior. The solutions, which are close to solutions in the tabu list, are systematically eliminated. The objective function to be minimized is evaluated for the new solutions and the best one becomes the new current solution s, even if the objective function is worse than the previous value. After each move, s is put into the tabu list.

In the diversification phase TS generates a list of promising solutions to locate the regions of the search domain which correspond to low values of the function to be minimized. Each current solution s is inserted into the promising list if the objective function is lower than a given threshold. Each solution in the promising

list can be considered as the center of a hypersphere called promising area. New solutions are added to the list only if they do not belong to any of the promising hyperspheres. This condition stimulates the search toward new areas of the domain.

After the diversification phase, the individuals of the promising list, ordered according to the objective function, are copied into the initial populations of GA, DE, and PSO until the population is completed (number of individuals in the algorithm population smaller than number of individuals in the promising list) or the promising list is totally exploited (in the opposite case); in the latter case the each algorithm initial population is completed with individuals created randomly. The exchange process between the different algorithms is clonation.

2.4 Indirect Method Optimization

In this thesis an Indirect Method for trajectory optimization is used and it will be described in details in this paragraph. The statement of the optimization problem is the one exposed at the beginning of the chapter, but some parts will be repeated for the sake of clarity. The time t is the independent variable, $\boldsymbol{x}$ is the vector of the state variables (n-component vector) and $\boldsymbol{u}$ is the control vector (q-component vector), while $\boldsymbol{\psi} = 0$ is the m-component vector of constraints.

The Bolza problem, defined as sum of Mayer (2.5) and Lagrangian (2.6) performance index, consists in finding the extremal path $\boldsymbol{x}(t)$ and the corresponding optimal control law $\boldsymbol{u}(t)$ that satisfy the differential equation $\dot{\boldsymbol{x}}(t) = \boldsymbol{f}(\boldsymbol{x},\boldsymbol{u},t)$ and the boundary equations, maximizing (or minimizing) the performance index J.

The trajectory is split in j phases and each point is labeled by the time t_j, where the state variable vector assume values $\boldsymbol{x}_j$ (the subscript here indicates the point and not the variable inside the state variable vector). Each point is called joining or internal boundary point. The variables can have different values before and after the point, so that discontinuity can be handled.

The j-th interval goes from $t_{(j-1)_+}$ to $t_{(j)_-}$ and the variable values at the extremities are indicated as $\boldsymbol{x}_{(j-1)_+}$ to $\boldsymbol{x}_{(j)_-}$, with $j = 1,..,f$, where f is the number of phases.

The Bolza problem performance index is (compare (2.5) and (2.6))

$$J = \phi(\boldsymbol{x}_0,\boldsymbol{x}_{1\pm},...,\boldsymbol{x}_f,t_0,t_{1\pm},...,t_f) + \sum_{j=i}^{f} \int_{t_{(j-1)+}}^{t_{(j)-}} \Phi(\boldsymbol{x},\dot{\boldsymbol{x}},t)\mathrm{dt} \tag{2.25}$$

and the boundary conditions are written as

$$\boldsymbol{\psi}(\boldsymbol{x}_{(j-1)_+},\boldsymbol{x}_{j_-},t_{(j-1)_+},t_{j_-}) = 0 \qquad j = 1,\ldots,f \tag{2.26}$$

,

In the code developed at Politecnico di Torino only Mayer formulation is used. J is a functional and the calculus of variations is used to study the behavior of the performance index given its variables. The Optimal Control Theory OCT [53] is the theory that uses calculus of variations to maximize or minimize a functional. The maximization problem can be changed into a minimization problem changing the sign of ϕ and Φ, and here only the maximization problem is considered.

In the Bolza problem 2.25 there are not reference to the boundary conditions or the differential equations, but an augmented index can be introduced:

$$J^* = \phi + \boldsymbol{\mu}\boldsymbol{\psi} + \sum_{j=i}^{f} \int_{t_{(j-1)+}}^{t_{(j)-}} [\Phi + \boldsymbol{\lambda}^T(\boldsymbol{f} - \dot{\boldsymbol{x}})]\mathrm{dt} \tag{2.27}$$

The new variables added are the adjoint variables $\boldsymbol{\lambda}$ (n-component vector) and the adjoint constants $\boldsymbol{\mu}$. The adjoint variables are associated with the state variables, while adjoint constants are associated with the constraints. When Boundary conditions and differential equation are satisfied (the solution is feasible), $J = J^*$ for any choice of $\boldsymbol{\lambda}$ and $\boldsymbol{\mu}$.

The behavior of J^* can be analyzed by the first order expansion of the functional. In the subsequent expression the interior point are omitted in order to improve clearness and they will be re-introduce later.

$$\begin{aligned}
\mathrm{dJ}^* &= \left(\frac{\partial\phi}{\partial t_f} + \boldsymbol{\mu}^T\frac{\partial\psi}{\partial t_f} + \Phi_f + \boldsymbol{\lambda}_f^T(\boldsymbol{f}_f - \dot{\boldsymbol{x}}_f)\right)\mathrm{dt_f} + \\
&+ \left(\frac{\partial\phi}{\partial t_0} + \boldsymbol{\mu}^T\frac{\partial\psi}{\partial t_f} - \Phi_0 - \boldsymbol{\lambda}_0^T(\boldsymbol{f}_0 - \dot{\boldsymbol{x}}_0)\right)\mathrm{dt_0} + \\
&+ \left(\frac{\partial\phi}{\partial \boldsymbol{x}_f} + \boldsymbol{\mu}^T\frac{\partial\boldsymbol{\psi}}{\partial \boldsymbol{x}_f}\right)\mathrm{d}\boldsymbol{x}_\mathrm{f} + \\
&+ \left(\frac{\partial\phi}{\partial \boldsymbol{x}_0} + \boldsymbol{\mu}^T\frac{\partial\boldsymbol{\psi}}{\partial \boldsymbol{x}_0}\right)\mathrm{d}\boldsymbol{x}_0 + \\
&+ \int_{t_0}^{t_f}\left[\frac{\partial(\Phi + \boldsymbol{\lambda}^T\boldsymbol{f})}{\partial\boldsymbol{x}}\delta\boldsymbol{x} + \frac{\partial(\Phi + \boldsymbol{\lambda}^T\boldsymbol{f})}{\partial\boldsymbol{u}}\delta\boldsymbol{u} - \boldsymbol{\lambda}^T\delta\dot{\boldsymbol{x}}\right]\mathrm{dt}
\end{aligned} \tag{2.28}$$

The Hamiltonian defined as $H = \Phi + \boldsymbol{\lambda}^T\boldsymbol{f}$ is introduced and substituted in 2.28. Considering that

$$\mathrm{d}\boldsymbol{x} = \delta\boldsymbol{x} + \dot{\boldsymbol{x}}\mathrm{dt} \tag{2.29}$$

and integrating $\delta\dot{\boldsymbol{x}}$ by parts

$$\int_{t_0}^{t_f} -\boldsymbol{\lambda}^T\delta\dot{\boldsymbol{x}}\mathrm{dt} = -\boldsymbol{\lambda}_\mathrm{f}^\mathrm{T}\delta\boldsymbol{x}_\mathrm{f} + \boldsymbol{\lambda}_0^\mathrm{T}\delta\boldsymbol{x}_0 + \int_{t_0}^{t_f} -\dot{\boldsymbol{\lambda}}^\mathrm{T}\delta\boldsymbol{x}\mathrm{dt} \tag{2.30}$$

the first variation of J^* can be written now as

$$\begin{aligned} \mathrm{dJ}^* &= \left(\frac{\partial \phi}{\partial t_f} + \boldsymbol{\mu}^T \frac{\partial \psi}{\partial t_f} + H_f\right) \mathrm{dt_f} + \\ &+ \left(\frac{\partial \phi}{\partial t_0} + \boldsymbol{\mu}^T \frac{\partial \psi}{\partial t_f} - H_0\right) \mathrm{dt}_0 + \\ &+ \left(-\boldsymbol{\lambda}_f + \frac{\partial \phi}{\partial \boldsymbol{x}_f} + \boldsymbol{\mu}^T \frac{\partial \boldsymbol{\psi}}{\partial \boldsymbol{x}_f}\right) \mathrm{d}\boldsymbol{x}_\mathrm{f} + \\ &+ \left(\boldsymbol{\lambda}_0 + \frac{\partial \phi}{\partial \boldsymbol{x}_0} + \boldsymbol{\mu}^T \frac{\partial \boldsymbol{\psi}}{\partial \boldsymbol{x}_0}\right) \mathrm{d}\boldsymbol{x}_0 + \\ &+ \int_{t_0}^{t_f} \left[\left(\frac{\partial H}{\partial \boldsymbol{x}} + \dot{\boldsymbol{\lambda}}^T\right) \delta \boldsymbol{x} + \frac{\partial H}{\partial \boldsymbol{u}} \delta \boldsymbol{u}\right] \mathrm{dt} \end{aligned} \tag{2.31}$$

The necessary condition for the stationarity of the performance index J is that $\mathrm{dJ} = 0$ for any admissible variation which is guaranteed by posing $\mathrm{dJ}^* = 0$ for any choice of $\delta\boldsymbol{x}$, $\delta\boldsymbol{u}$, $\mathrm{d}\boldsymbol{x}_\mathrm{f}$,$\mathrm{d}\boldsymbol{x}_0$,$\mathrm{dt_f}$, dt_0. The adjective admissible means that each choice must fulfill the boundary conditions and the differential equations. The first order variation is null when all the coefficients of the admissible choices are nullified. In other words $\boldsymbol{\lambda}$ and $\boldsymbol{\mu}$ can be chosen in order to have $\mathrm{dJ}^* = 0$ whatever values take $\delta\boldsymbol{x}$, $\delta\boldsymbol{u}$, $\mathrm{d}\boldsymbol{x}_\mathrm{f}$,$\mathrm{d}\boldsymbol{x}_0$,$\mathrm{dt_f}$, dt_0.

Nullifying the coefficient of $\delta\boldsymbol{x}$ gives the Euler-Lagrange equations

$$\frac{\mathrm{d}\boldsymbol{\lambda}}{\mathrm{dt}} = -\left(\frac{\partial H}{\partial \boldsymbol{x}}\right)^T \tag{2.32}$$

that is a set of n differential equations that describes how the adjoint variables evolve during the trajectory.

Nullifying $\delta\boldsymbol{u}$ provides q algebraic equations

$$\left(\frac{\partial H}{\partial \boldsymbol{u}}\right)^T = 0 \tag{2.33}$$

that define the optimal control values. They do not formally depend on the performance index.

The other coefficients are related to the initial and final conditions, but it is better to introduce the interior point constraints for having a more general framework. Rewriting 2.31 with the interior point constraints

$$
\begin{aligned}
\mathrm{dJ}^* &= \sum_{j=0}^{f}[\left(\frac{\partial\phi}{\partial t_{j-}}+\boldsymbol{\mu}^T\frac{\partial\psi}{\partial t_{j-}}+H_{j-}\right)\mathrm{dt_{j-}}+\\
&+ \left(\frac{\partial\phi}{\partial t_{j+}}+\boldsymbol{\mu}^T\frac{\partial\psi}{\partial t_{j+}}-H_{j+}\right)\mathrm{dt_{j+}}+\\
&+ \left(-\boldsymbol{\lambda}_{j-}+\frac{\partial\phi}{\partial \boldsymbol{x}_{j-}}+\boldsymbol{\mu}^T\frac{\partial\boldsymbol{\psi}}{\partial \boldsymbol{x}_{j-}}\right)\mathrm{d}\boldsymbol{x}_{\mathrm{j-}}+\\
&+ \left(\boldsymbol{\lambda}_{j+}+\frac{\partial\phi}{\partial \boldsymbol{x}_{j+}}+\boldsymbol{\mu}^T\frac{\partial\boldsymbol{\psi}}{\partial \boldsymbol{x}_{j+}}\right)\mathrm{d}\boldsymbol{x}_{\mathrm{j+}}]+\\
&+ \sum_{j=1}^{f}\int_{t_{(j-1)+}}^{t_{j-}}\left[\left(\frac{\partial H}{\partial \boldsymbol{x}}+\dot{\boldsymbol{\lambda}}^T\right)\delta\boldsymbol{x}+\frac{\partial H}{\partial \boldsymbol{u}}\delta\boldsymbol{u}\right]\mathrm{dt} \qquad (2.34)
\end{aligned}
$$

The conditions for nullifying the coefficients of $\mathrm{d}\boldsymbol{x}_{\mathrm{j-}}$ and $\mathrm{d}\boldsymbol{x}_{\mathrm{j+}}$ are called conditions for optimality. At generic point j (end of phase j and at the beginning of phase $j+1$) they are:

$$
\begin{aligned}
-\boldsymbol{\lambda}_{j-}^T+\frac{\partial\phi}{\partial \boldsymbol{x}_{j-}}+\boldsymbol{\mu}^T\left[\frac{\partial\boldsymbol{\psi}}{\partial \boldsymbol{x}_{j-}}\right] &= 0 \qquad j=1,\ldots,f \qquad (2.35)\\
\boldsymbol{\lambda}_{j+}^T+\frac{\partial\phi}{\partial \boldsymbol{x}_{j+}}+\boldsymbol{\mu}^T\left[\frac{\partial\boldsymbol{\psi}}{\partial \boldsymbol{x}_{j+}}\right] &= 0 \qquad j=0,\ldots,f-1 \qquad (2.36)
\end{aligned}
$$

The transversality conditions are the ones for nullifying the coefficients dt

$$
\begin{aligned}
H_{j-}+\frac{\partial\phi}{\partial t_{j-}}+\boldsymbol{\mu}^T\frac{\partial\boldsymbol{\psi}}{\partial t_{j-}} &= 0 \qquad j=1,\ldots,f \qquad (2.37)\\
-H_{j+}+\frac{\partial\phi}{\partial t_{j+}}+\boldsymbol{\mu}^T\frac{\partial\boldsymbol{\psi}}{\partial t_{j+}} &= 0 \qquad j=0,\ldots,f-1 \qquad (2.38)
\end{aligned}
$$

It is possible to see that the shape of the transversality conditions is very similar to the optimality conditions. The Hamiltonian seems to have the same function for the time that the adjoint variables have for state variables.

The Hamiltonian is a function with interesting properties. If its time derivative is observed

$$
\frac{\mathrm{dH}}{\mathrm{dt}}=\frac{\partial H}{\partial t}+\frac{\partial H}{\partial \boldsymbol{x}}\dot{\boldsymbol{x}}+\frac{\partial H}{\partial \boldsymbol{\lambda}}\dot{\boldsymbol{\lambda}}+\frac{\partial H}{\partial \boldsymbol{u}}\dot{\boldsymbol{u}} \qquad (2.39)
$$

and considering that $(\partial H/\partial\lambda)^T=\boldsymbol{f}=\dot{\boldsymbol{x}}$ and $\dot{\boldsymbol{\lambda}}=-(\partial H/\partial \boldsymbol{x})^T$, the Hamiltonian time derivative can be written as

$$\frac{\mathrm{dH}}{\mathrm{dt}} = \frac{\partial H}{\partial t} + \frac{\partial H}{\partial \boldsymbol{u}}\dot{\boldsymbol{u}} \tag{2.40}$$

so if the Hamiltonian does not explicitly depend on time ($\frac{\partial H}{\partial t} = 0$) and the optimal control law is adopted ($\frac{\partial H}{\partial \boldsymbol{u}} = 0$), the Hamiltonian is constant. This is a fast and simple check to find errors in the implementation of the optimal control theory in a real problem.

Optimality and transversality conditions depend on performance index and constraints. These conditions give the values (or the relationship between them) of the adjoint variables and constants. The possible constraints are infinite, but it is possible to see the most relevant conditions.

If the value of the variable x_i (x_i is the component i of vector $\boldsymbol{x}$, while $(x_i)_j$ is x_i at point j) is assigned at the beginning or at the end of the trajectory, the corresponding adjoint variable at that time is free. If the value of x_i is not assigned and the performance index does not depends on this variable at this time, the corresponding adjoint variable at the assigned time is set to zero.

If the constraint is applied at one interior point, there is a condition before the point (j_-) and after the point (j_+). If the variable is continuous and the value is assigned at the point j, the corresponding adjoint variable has a free discontinuity

$$(\lambda_i)_{j+} - (\lambda_i)_{j-} = -(\mu_1 + \mu_2) \tag{2.41}$$

while if the variable is continuous but unspecified, the corresponding adjoint variables is continuous.

The Hamiltonian has the same structure: it is continuous if the time at point j is free, while it has a jump if the time is assigned. If the final time is free, $H_f = 0$. In 4.1 the indirect method will be applied to the specific case of this thesis and more practical examples about optimal boundary conditions will be given.

The condition which states $\mathrm{dJ}^* = 0$, and so the optimality and transversality conditions, is useful for finding a stationary point, but it is necessary also to determine the nature of the stationary point. For understanding the nature of the point the second variation of J^* has to be analyzed.

In order to have a maximum the value of H_{uu} has to be negative definite (or positive definite if a minimum is searched). This is a necessary condition.

If the optimal path is supposed unique, for a given point $\boldsymbol{x}_0$, t_0 and constraints $\boldsymbol{\psi} = 0$, the optimal path provides the maximum index $J = J^0$ with control variable $\boldsymbol{u}^0(t)$. The Hamiltonian-Jacobi theory provides differential equations concerning J^0 and the optimal control $\boldsymbol{u}^0$, extended by Bellman to discrete systems. The practical implementation of this theory is known as dynamic programming. The Hamiltonian-Jacobi theory says that, given $\boldsymbol{x}$,$\boldsymbol{\lambda}$ and t, H has to be maximized with respect to $\boldsymbol{u}$ in order to have J^0. The same result was obtained independently by Pontryagin

and it is known as Pontryagin's maximum principle (PMP). Without bounds on state and control variables, the maximization of H implies $H_u = 0$ and H_{uu} negative definite (local conditions). This means that if H is linear with respect to a control variable u_j, $\frac{\partial H}{\partial u_j} = 0$ does not contain u_j, that is, it is indeterminate. The problem has a solution only if u_j is bounded. In this case the optimal control value is the one that maximizes H. This is called Bang-Bang control.

The Optimal Control Theory exposed here formulates a multi-point boundary value problem (BVP), where some state values, adjoint variables and constants are unknowns. The unknown values can be found at the internal point, or at the beginning or ending point of the trajectory. The OCT provides the optimal boundary conditions that must be added to the constraints of the problem. The constant Lagrange multipliers $\boldsymbol{\mu}$ are eliminated from Eqs. (2.35)-(2.38); the resulting boundary conditions for optimality and the boundary conditions on the state variables, given by Eq. (2.26), are collected in a single vector in the form

$$\boldsymbol{\sigma}(\boldsymbol{x}_{(j-1)_+},\boldsymbol{x}_{j_-},\boldsymbol{\lambda}_{(j-1)_+},\boldsymbol{\lambda}_{j_-},t_{(j-1)_+},t_{j_-}) = 0 \qquad j = 1,\ldots,f \tag{2.42}$$

All these conditions must be satisfied at the relevant points.

The optimization problem state at the beginning of this chapter, subjected to ODE 2.1 and to constraints 2.2, is now a BVP where ODE are integrated and the boundary conditions are evaluated after each integration. The solution of BVP is found through iterative solution of an initial value problem (IVP) where initial values of all variables and constant parameters are considered as given. The iterative procedure is based on Newton's method.

The differential equations are integrated by a multistep implicit method, with variable step and order, based on Adam-Moulton method [54]- [55].

As said before, the independent variable is the time t. The trajectory is divided in phases, but the duration τ_j of each phase is unknown. So an independent variable transformation is introduced. The new independent variable is ϵ and its value at the j-th arc is

$$\epsilon = j - 1 + \frac{t - t_{j-1}}{t_j - t_{j-1}} = j - 1 + \frac{t - t_{j-1}}{\tau_j} \tag{2.43}$$

At the j-th arc the value of ϵ varies between j-th and j. The ODE are transformed in

$$\frac{\mathrm{d}\boldsymbol{x}}{\mathrm{d}\epsilon} = \tau_j \frac{\mathrm{d}\boldsymbol{x}}{\mathrm{dt}} \tag{2.44}$$

$$\frac{\mathrm{d}\boldsymbol{\lambda}}{\mathrm{d}\epsilon} = \tau_j \frac{\mathrm{d}\boldsymbol{\lambda}}{\mathrm{dt}} \tag{2.45}$$

The constant parameters are collected in the $\boldsymbol{y}$ vector and the equation is $(\mathrm{d}\boldsymbol{y}/\mathrm{d}\epsilon) = 0$. All the variables are collected in a single vector $\boldsymbol{z}$

$$\boldsymbol{z} = \begin{pmatrix} \boldsymbol{x} \\ \boldsymbol{\lambda} \\ \boldsymbol{y} \end{pmatrix} \tag{2.46}$$

and the differential equations are generally indicated as

$$\frac{\partial \boldsymbol{z}}{\partial \epsilon} = \boldsymbol{g}(\boldsymbol{z},\epsilon) \tag{2.47}$$

Variable value at the relevant boundaries are collected in the vector

$$\boldsymbol{s} = (\boldsymbol{z}_{0+},\boldsymbol{z}_{1\pm},\ldots,\boldsymbol{z}_{(f-1)\pm},\boldsymbol{z}_f) \tag{2.48}$$

and the boundary condition can be written in a synthetic way as

$$\Psi(\boldsymbol{s}) = 0 \tag{2.49}$$

The unknown initial values and parameters are collected into vector $\boldsymbol{p}$ and the first tentative guess is $\boldsymbol{p}^0$. Posing $\boldsymbol{z}_0 = \boldsymbol{p}^0$, the differential equations are integrated and the boundary conditions $\Psi(\boldsymbol{s})$ are evaluated. To reduce the errors at bounds the parameters have to be changed. At the r-th iteration the parameters will be

$$\boldsymbol{p}^{r+1} = \boldsymbol{p}^r + \Delta\boldsymbol{p} \tag{2.50}$$

At first orders, to choose how much the parameters have to change, the matrix of the derivative of the errors with respect to the parameters can be used.

$$\Delta\boldsymbol{p} = \boldsymbol{p}^{r+1} - \boldsymbol{p}^r = -\left[\frac{\partial \boldsymbol{\Psi}}{\partial \boldsymbol{p}}\right]^{-1} \boldsymbol{\Psi}^r \tag{2.51}$$

The matrix $[\partial\boldsymbol{\Psi}/\partial\boldsymbol{p}]$ has to be non-singular and can be evaluated numerically or analytically. For the computation in the analytic shape, the matrix is decomposed in

$$\left[\frac{\partial \boldsymbol{\Psi}}{\partial \boldsymbol{p}}\right] = \left[\frac{\partial \boldsymbol{\Psi}}{\partial \boldsymbol{s}}\right]\left[\frac{\partial \boldsymbol{s}}{\partial \boldsymbol{p}}\right] \tag{2.52}$$

The matrix $[\partial\boldsymbol{\Psi}/\partial\boldsymbol{s}]$ is obtained by derivation of the boundary conditions, while the matrix $[\partial\boldsymbol{s}/\partial\boldsymbol{p}]$ collects the values at boundaries of the matrix $[\partial\boldsymbol{z}/\partial\boldsymbol{p}]$. In other words:

$$\left[\frac{\partial \boldsymbol{s}}{\partial \boldsymbol{p}}\right] = \left[\frac{\partial \boldsymbol{z}_0}{\partial \boldsymbol{p}} \; \frac{\partial \boldsymbol{z}_1}{\partial \boldsymbol{p}} \ldots\right] \tag{2.53}$$

The matrix is obtained by integration of the homogeneous differential system

$$\left[\frac{\partial \dot{\boldsymbol{z}}}{\partial \boldsymbol{p}}\right] = \left[\frac{\partial \boldsymbol{g}}{\partial \boldsymbol{z}}\right]\left[\frac{\partial \boldsymbol{z}}{\partial \boldsymbol{p}}\right] \tag{2.54}$$

In this thesis the matrix $[\partial\boldsymbol{\Psi}/\partial\boldsymbol{p}]$ is evaluated only numerically. Each parameter p_i is in turn varied by a small quantity δp_i around the value of the previous iteration p_i^r. The small quantity is generally 10^{-5}, but it can be changed depending on the nature of the problem. If it is too large or too small the linearization is not able to catch the local shape of the errors. The differential equations are integrated and the changes of variable values are evaluated at relevant points $\delta\boldsymbol{s}$. The changes in error on boundary conditions are $\delta\boldsymbol{\Psi}$. The i-th column of $[\partial\boldsymbol{\Psi}/\partial\boldsymbol{p}]$ is approximate by linearization as

$$\left[\frac{\partial \boldsymbol{\Psi}}{\partial p_i}\right] = \frac{\delta \boldsymbol{\Psi}}{\delta p_i} \tag{2.55}$$

The linearization of the matrix $[\partial\boldsymbol{\Psi}/\partial\boldsymbol{p}]$ introduce errors in the evaluation of the matrix itself. These errors can prevent convergence, so $\Delta\boldsymbol{p}$ is modified from equation (2.51). There two ways for improving the stability of the procedure. The first one is to check the error variation between two different iterations.

If $max(\boldsymbol{\Psi}^{r+1}) > k_1 max(\boldsymbol{\Psi}^r)$ than the correction $\Delta\boldsymbol{p}$ is halved and results $\boldsymbol{p}^{r+1} = \boldsymbol{p}^r + \Delta\boldsymbol{p}/2$. This operation is generally called bisection and the bisection parameter k_1 is usually posed equal to 2. This value generally provides good results also because it permits a limited increase of the maximum error and so the indirect method can exit from a local minimum valley.

The second operation is to use a reduced parameter correction

$$\Delta\boldsymbol{p} = -k_2 \left[\frac{\partial \boldsymbol{\Psi}}{\partial \boldsymbol{p}}\right]^{-1} \boldsymbol{\Psi}^r \tag{2.56}$$

This parameter is the scalar step length and the value is usually set in the range $0.01 \leq k_2 \leq 1$ as input of the program and it is not found by a line search.

Conclusions

The definition of a general optimization problem and its taxonomy has been given in this chapter. In space trajectory optimization direct, indirect and evolutionary methods are mainly used. Today also differential dynamic programming is successfully used in this field. Direct methods can deal easily with many problems, considering equality and inequality constraints. They have also a greater convergence radius with respect to indirect methods. The number of unknowns is large

and the solution of this problem is numerically demanding. They rely on a tentative solution.

Evolutionary methods are simple to apply and they can virtually find a global optimum, but they require a great number of function evaluations, so they are mainly used with approximate model.

Indirect methods are fast and give insight of the problems. They have small convergence radius, they rely on tentative solution and they cannot solve the optimization problem as a black box. Euler-Lagrange equations are derived together with optimality and transversality conditions. The Boundary Value Problem (BVP) and its solution by the procedure developed at "Politecnico di Torino" has been exposed. The procedure try to overcome the issues coming from the small convergence radius typical of indirect methods.

Chapter 3

Dynamic Model

Introduction

Different forces act on the spacecraft: Earth, Sun and Moon gravity, thrust and solar radiation pressure. The dynamic model considering the two body problem, the thrust control and the above mentioned perturbations will be described in this chapter. The Hamiltonian and the differential equations of state and adjoint variables will be derived in a topocentric frame.

3.1 Differential equations and reference frame

In Chapter 2 the main methods used in astrodynamics optimization have been briefly introduced and the indirect method used in thesis was deeply studied. Before starting with the case study, it is important to introduce the dynamic model. This thesis topic is the optimization of deployment trajectories of a couple of spacecrafts, but the dynamic model is the same for both, so all the considerations made for one satellite are valid for the other one. First the state $\boldsymbol{x}$ and control $\boldsymbol{u}$ vectors are defined. Trajectory is the evolving of the position of the spacecraft during time and so the natural state vector is made up by the position vector $\boldsymbol{r}$ and the velocity vector $\boldsymbol{V}$. In order to complete the state vector also the mass m, which is a scalar quantity, is introduced. The attitude of the spacecraft, even if it will be considered in some assumptions later, is not considered in the optimization process, so the spacecraft is assumed as a point mass. The control is the vector $\boldsymbol{T}$, that can vary in magnitude and direction. It section 4.2 is explained that thrust magnitude will be either maximum or minimum in order to fulfill optimality condition.

The simplest model used in preliminary design analysis is the two body model. It is possible to find reference in many basic books of Astrodynamics or physics, such as Bate [56]. In this model the assumption are

- the spacecraft mass is negligible respect to central body mass
- the central body has a spherical mass distribution or the spacecraft is far enough, in order to consider all the mass as a point

In the two-body model only the gravitational force of the main body is considered.

This model is a good first approximation, but it is far enough from the reality, i.e. if a Low Earth orbit or HEO is considered. In space environment there are different types of perturbations that must be taken in account, depending on which problem is considered.

In this thesis the two body problem approximation plus perturbations are considered as dynamical force. Before going in details it is possible to write the differential equation of the state vector written in vectorial form.

$$\begin{aligned} \mathrm{d}\boldsymbol{r}/\mathrm{d}t &= \boldsymbol{V} && (3.1)\\ \mathrm{d}\boldsymbol{V}/\mathrm{d}t &= -\mu\boldsymbol{r}/r^3 + \boldsymbol{T}/m + \boldsymbol{a}_p && (3.2)\\ \mathrm{d}m/\mathrm{d}t &= -T/c && (3.3) \end{aligned}$$

where $-\mu\boldsymbol{r}/r^3$ is the central body spherical gravitational acceleration, while $\boldsymbol{a}_p$ collects the perturbing accelerations. In the mass differential equation c is the effective gas exhaust velocity (in literature is indicated also as v_e). T/c is the mass flow. As said before, the thrust vector is the only control of the trajectory and can vary its magnitude between maximum and minimum values. The specific impulse, and so c, is considered constant in this problem.

In the specific problem of orbital transfer between elliptic orbit, the central body is the Earth and the perturbations, which are considered in this work are:

$$\boldsymbol{a}_p = \boldsymbol{a}_J + \boldsymbol{a}_{lsg} + \boldsymbol{a}_{srp} \tag{3.4}$$

where $\boldsymbol{a}_J$ are the perturbations due to Earth asphericity, $\boldsymbol{a}_{lsg}$ are the gravitational forces of "'third bodies"', in particular the subscript l indicates the lunar perturbation, while s indicates solar ones. $\boldsymbol{a}_{srp}$ represents the perturbations due to solar radiation pressure, that is the pressure of the photons coming from the Sun. The Earth Mean Equator and Equinox of Epoch J2000 (i.e. EME2000) reference frame is adopted. In this reference frame the unit vectors are indicated as $\boldsymbol{I}$, $\boldsymbol{J}$, $\boldsymbol{K}$. The first vector points towards the Vernal Equinox, the third is perpendicular to the ecliptic plane and points towards the celestial North Pole, and the second one is chosen in order to have a right hand frame. Precession and nutation are neglected. Position is described by radius r, right ascension ϑ and declination φ. The position vector in the inertial frame can be written as

$$\boldsymbol{r} = r\cos\vartheta\cos\varphi\boldsymbol{I} + r\sin\vartheta\cos\varphi\boldsymbol{J} + r\sin\varphi\boldsymbol{K} \tag{3.5}$$

and the length element can be written as

$$\mathrm{d}l^2 = \mathrm{d}r^2 + (rcos\varphi)^2\mathrm{d}\vartheta^2 + r^2\mathrm{d}\varphi^2 \tag{3.6}$$

A topocentric frame defined by unit vector $\boldsymbol{\imath}$ (radial), $\boldsymbol{\jmath}$ (eastward), and $\boldsymbol{k}$ (northward) is also introduced (Fig. 3.1). The transition matrix from inertial to topocentric coordinates is

$$\begin{Bmatrix} \boldsymbol{\imath} \\ \boldsymbol{\jmath} \\ \boldsymbol{k} \end{Bmatrix} = \begin{bmatrix} \cos\vartheta\cos\varphi & \sin\vartheta\cos\varphi & \sin\varphi \\ -\sin\vartheta & \cos\vartheta & 0 \\ -\cos\vartheta\sin\varphi & -\sin\vartheta\sin\varphi & \cos\varphi \end{bmatrix} \begin{Bmatrix} \boldsymbol{I} \\ \boldsymbol{J} \\ \boldsymbol{K} \end{Bmatrix} \tag{3.7}$$

In the topocentric frame the position vector is simply

$$\boldsymbol{r} = r\boldsymbol{i} \tag{3.8}$$

while the velocity vector is split in three components

$$\boldsymbol{v} = \dot{\boldsymbol{r}} = u\boldsymbol{\imath} + v\boldsymbol{\jmath} + w\boldsymbol{k} \tag{3.9}$$

with u, v, and w radial, eastward and northward components, respectively. The spherical symmetry of the gravitational field of the two body problems (that is the main contribution in the dynamic of the problem) makes the choice of spherical coordinates and topocentric velocity components almost natural. The velocity vector written in topocentric frame is also more intuitive than in rectangular coordinates based on inertial frame. Dynamic equations are also easier to understand because gravity of the central body acts only on the radial component of velocity and the others contributions are centrifugal and Coriolis force components. The advantage is mainly numeric, because $u \approx 0$ and r is approximately constant.

The same problem has been solved using also equinoctial equations [57] [12], but the derivation of the optimal conditions is more difficult and the computational time for the single solution is higher. Generally, these state variables are useful to understand the behavior of the osculating orbit (more than the motion of the spacecraft), but they give some issues in the derivation of perturbations components and the necessary optimal conditions/Euler-Lagrange equations for the indirect method formulation. The scalar dynamic equation are expressed, in the topocentric frame,

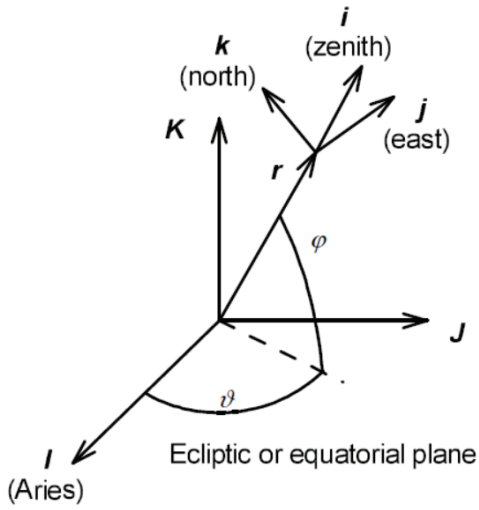

Figure 3.1: Spherical Reference frame

as

$$
\begin{aligned}
\mathrm{d}r/\mathrm{d}t &= u && (3.10)\\
\mathrm{d}\vartheta/\mathrm{d}t &= v/(r\cos\varphi) && (3.11)\\
\mathrm{d}\varphi/\mathrm{d}t &= w/r && (3.12)\\
\mathrm{d}u/\mathrm{d}t &= -\mu/r^2 + (v^2+w^2)/r + T_u/m + (a_p)_u && (3.13)\\
\mathrm{d}v/\mathrm{d}t &= (-uv + vw\tan\varphi)/r + T_v/m + (a_p)_v && (3.14)\\
\mathrm{d}w/\mathrm{d}t &= (-uw - v^2\tan\varphi)/r + T_w/m + (a_p)_w && (3.15)\\
\mathrm{d}m/\mathrm{d}t &= -T/c && (3.16)
\end{aligned}
$$

where subscripts u, v, and w denote the components along $\boldsymbol{\imath}$, $\boldsymbol{\jmath}$, and $\boldsymbol{k}$, respectively. In the derivation of the scalar equation of the spherical coordinates it should be paid attention to the metric of the spherical coordinates that comes from the length element equation 3.6. Also different perturbations can be taken in account.

In the following paragraphs a deeper analysis of the perturbations is carried on. Now that the dynamic equation are defined it is possible to write the Euler-Lagrange equations (2.32). First the Hamiltonian has to be written. In the vectorial form is

quite simple.

$$
\begin{aligned}
H &= \boldsymbol{\lambda}^T \dot{\boldsymbol{x}} = H_{2B} + H_T + H_p && (3.17)\\
H_{2B} &= \boldsymbol{\lambda}_r^T \boldsymbol{V} + \boldsymbol{\lambda}_V^T \boldsymbol{g} && (3.18)\\
H_T &= \boldsymbol{\lambda}_V^T \boldsymbol{T}/m - \lambda_m (T/c) && (3.19)\\
H_p &= \boldsymbol{\lambda}_V^T \boldsymbol{a}_p = H_J + H_{lsg} + H_{srp} && (3.20)\\
H_J &= \boldsymbol{\lambda}_V^T \boldsymbol{a}_J && (3.21)\\
H_{lsg} &= \boldsymbol{\lambda}_V^T \boldsymbol{a}_{lsg} && (3.22)\\
H_{srp} &= \boldsymbol{\lambda}_V^T \boldsymbol{a}_{srp} && (3.23)
\end{aligned}
$$

and Euler-Lagrange equations are written (if thrust is independent of state variables) as

$$
\begin{aligned}
\mathrm{d}\boldsymbol{\lambda}_r/\mathrm{d}t &= (\partial \boldsymbol{g}/\partial \boldsymbol{r} + \partial \boldsymbol{a}_p/\partial \boldsymbol{r})^T \boldsymbol{\lambda}_V && (3.24)\\
\mathrm{d}\boldsymbol{\lambda}_V/\mathrm{d}t &= -\boldsymbol{\lambda}_r && (3.25)\\
\mathrm{d}\lambda_m/\mathrm{d}t &= \boldsymbol{\lambda}_V \boldsymbol{T}/m^2 && (3.26)\\
& && (3.27)
\end{aligned}
$$

The subscripts J stands for geopotential perturbation, lsg for luni-solar gravity and srp stands for solar radiation pressure.

These equations have to be changed if thrust depends on radius, for example if the distance from the sun changes significantly, such as in an interplanetary mission, and the power of solar arrays drops down. In the topocentric reference frame and spherical coordinates the Hamiltonian is written

$$
\begin{aligned}
H = {} & \lambda_r u + \lambda_\vartheta v/(r\cos\varphi) + \lambda_\varphi w/r + \\
& + \lambda_u \left[-\mu/r^2 + (v^2+w^2)/r + (a_J)_u + (a_{lsp})_u + (a_{srp})_u\right] + \\
& + \lambda_v \left[(-uv + vw\tan\varphi)/r + (a_J)_v + (a_{lsp})_v + (a_{srp})_v\right] + \\
& + \lambda_w \left[(-uw - v^2\tan\varphi)/r + (a_J)_w + (a_{lsp})_w + (a_{srp})_w\right] + \\
& + \left((\lambda_u T_u + \lambda_v T_v + \lambda_w T_w)/m - \lambda_m (T/c)\right) \qquad (3.28)
\end{aligned}
$$

And scalar equations of Euler-Lagrange are

$$
\begin{aligned}
\mathrm{d}\lambda_r/\mathrm{d}t &= [\lambda_\vartheta(v/\cos\varphi) + \lambda_\varphi w + \lambda_u(-2\mu/r + v^2 + w^2) \\
&+ \lambda_v(-uv + vw\tan\varphi + \lambda_w(-uw - v^2\tan\varphi)]/r^2 + (\Delta\dot{\lambda}_p)_r && (3.29)\\
\mathrm{d}\lambda_\vartheta/\mathrm{d}t &= (\Delta\dot{\lambda}_p)_\vartheta && (3.30)\\
\mathrm{d}\lambda_\varphi/\mathrm{d}t &= (-\lambda_\vartheta v\sin\varphi - \lambda_v vw + \lambda_w v^2)/(r\cos^2\varphi) + (\Delta\dot{\lambda}_p)_\varphi && (3.31)\\
\mathrm{d}\lambda_u/\mathrm{d}t &= (-\lambda_r r + \lambda_v v + \lambda_w w)/r + (\Delta\dot{\lambda}_p)_u && (3.32)\\
\mathrm{d}\lambda_v/\mathrm{d}t &= [-\lambda_\vartheta/\cos\varphi - 2\lambda_u v + \lambda_v(u - w\tan\varphi) + 2\lambda_w v\tan\varphi]/r \\
&+ (\Delta\dot{\lambda}_p)_v && (3.33)\\
\mathrm{d}\lambda_w/\mathrm{d}t &= (-\lambda_\varphi - 2\lambda_u w - \lambda_v v\tan\varphi + \lambda_w u)/r + (\Delta\dot{\lambda}_p)_w && (3.34)\\
\mathrm{d}\lambda_m/\mathrm{d}t &= T\lambda_V/m^2 + (\Delta\dot{\lambda}_p)_m && (3.35)
\end{aligned}
$$

where $\lambda_V = \sqrt{\lambda_u^2 + \lambda_v^2 + \lambda_w^2}$ is the magnitude of the primer vector $\boldsymbol{\lambda_V}$. In the set of differential equations the term $\Delta\dot{\lambda}_p$ indicates the sum of the contributions of the perturbations

$$\Delta\dot{\boldsymbol{\lambda}} = \dot{\boldsymbol{\lambda}}_{2B} + \dot{\boldsymbol{\lambda}}_J + \dot{\boldsymbol{\lambda}}_{lsg} + \dot{\boldsymbol{\lambda}}_{srp} \tag{3.36}$$

The thrust vector components $\boldsymbol{T}$ are

$$
\begin{aligned}
T_u &= T\sin\gamma_T \\
T_v &= T\cos\gamma_T\cos\psi_T \\
T_w &= T\cos\gamma_T\sin\psi_T
\end{aligned}
\tag{3.37}
$$

The angles are shown in Fig, 3.2

All quantities have been made dimensionless using as reference length the Earth radius ($R_{conv} = 6378.1363\,\mathrm{km}$), as reference velocity $V_{conv} = \sqrt{\mu/R_{conv}}$, as mass $m = 1000\,\mathrm{kg}$. After that, the other dimensionless quantities (time, acceleration) have been derived. The gravitational parameter in adimensional form is $\mu = 1$.

3.2 Geopotential Model

The two body problem considers the central body as a point mass body or perfectly spherical symmetrical gravitational field. Even if this is a good assumption in a preliminary analysis, closer the spacecraft is to the central body, more important are the contributions of the non-homogeneous distribution of mass. These perturbations can also affect in significant way the spacecraft motion when the satellite keeps the same position relative to Earth for a long time, such as a geo-synchronous satellite.

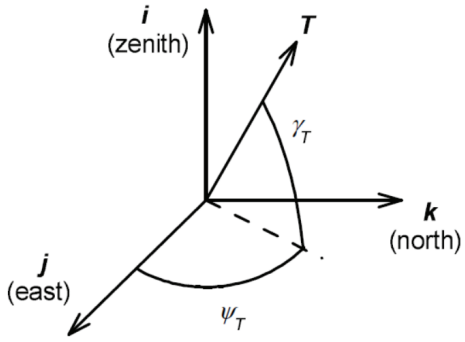

Figure 3.2: Thrust Direction

Giant planets such as Jupiter have a big oblateness perturbation and the problem of gravity asphericity is very challenging also for orbiting around bodies such as the Moon or for small bodies such asteroids. Probe Dawn found that Vesta asteroid has an unexpected tangential component of the gravitational field greater than the thrust its engines can provide.

Generally, this kind of perturbation are studied in preliminary analysis when considering the station keeping maneuver (often using equinoctial averaged equation), but the effects of asphericity perturbations can be important also in transfer problem.

The gravitational field is defined as an integral that is function of the mass distribution inside the body. When the body has spherical symmetry, the gravitational field and its acceleration are those described by the two-body problem. If the body is not spherical the gravitational field has different equipotential surfaces and the acceleration is no more radial. The difference between the gravity acceleration of the two-body model and the one found by the mass distribution is taken in account in the perturbation vector $\boldsymbol{a}_J$.

The potential field generated by a non spherical mass distribution can be expressed as series of spherical harmonics, where the first harmonic is the pure sphere and it is the same of two-body problem. The general theoretical frame is well described in [58] and the model is updated and verified during the years.

When real celestial bodies are considered, the real mass distribution is unknown. Gravitational field is measured considering deviation of satellites or other little bodies from the predicted orbit. The measures coming from the orbit determination are used for computing the coefficients of the spherical harmonics. The gravitational model used in this work is described in NIMA technical report [59] and expressed by coefficients of EGM2008. For the equations the same reference frame used for

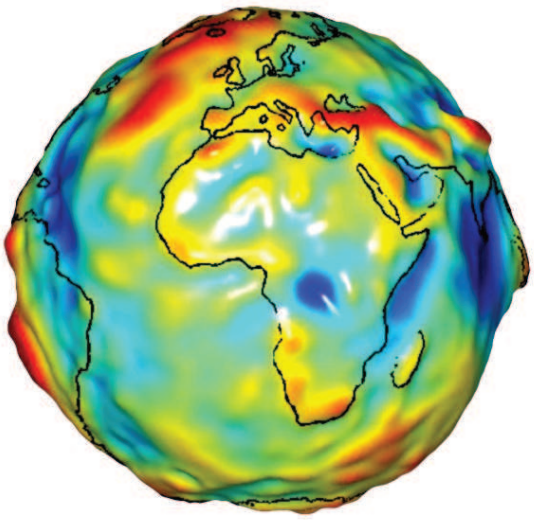

Figure 3.3: Image of Geoid. Credit: Grace/NASA

dynamic equation is adopted (EME2000) neglecting precession and nutation. In EGM2008 the geopotential is referred as

$$V = \mu/r + \Phi \tag{3.38}$$

with Φ

$$\Phi = -\mu/r \sum_{n=2}^{N} \left(\frac{r_E}{r}\right)^n \sum_{m=0}^{n} \left(C_{nm} \cos m\lambda + S_{nm} \sin m\lambda\right) P_{nm}(\sin \varphi) \tag{3.39}$$

where μ is the Earth gravitational parameter, r_E is the semimajor axis of the Earth ellipsoid. N is the number of the harmonics taken in consideration, while λ and φ are the longitude and latitude of the spacecraft respect to the Earth. It has to be noted that the latitude coincides with declination φ only because nutation is neglected. While longitude λ is related to right ascension ϑ by means of relation

$$\lambda = \vartheta - \vartheta_{G\text{ref}} - \omega_E(t - t_{\text{ref}}) \tag{3.40}$$

where $\vartheta_{G\text{ref}}$ is Greenwich right ascension at the reference time t_{ref} (51544.5 MJD) and ω_E is the angular velocity of the Earth's rotation. It is evaluated on the basis of the sidereal day (86164.098 s), neglecting precession and considering uniform rotation. The potential (3.39) is expressed as sum of spherical harmonics. The first harmonic is μ/r and is already considered in the two body dynamical problem. The

other harmonics are zonal and tesseral harmonics. The index n indicates the zonal ones, that are ondulation on latitude while the tesseral harmonics m superimpose on the previous ones. It is important to note the $m \leq n$. Coefficients C_{nm} and S_{nm} define the amplitude of this harmonics that are described by the associated Legendre functions P_{nm} and the combination of sine and cosine of λ and φ. These coefficients are taken from the EGM2008 model [60] and can be normalized or unnormalized. The first ones have a greater accuracy, while the second ones are faster (the normalization has to be recomputed at each derivation). Two types of models for coefficients can be used: the "'Tide Free"'and the "'Zero Tide"'. In this dissertion only the first one is used. The associated Legendre functions are solution of the Legendre equation. More information can be found in Abramowitz and Stegun [61], Bosch [62]. These functions can be computed iteratively or explicitly. In this study it is no necessary to go beyond 8x8 degrees in spherical harmonics, so it was preferred to write explicitly the functions in order to improve computational speed. For having more degrees it can be used the recursive functions.

$$
\begin{aligned}
t &= \sin\varphi && (3.41)\\
u &= \cos\varphi && (3.42)\\
P_{0,0}(t) &= 1 && (3.43)\\
P_{n+1,0}(t) &= (2n+1)tP_{n,0}(t) - nP_{n-1,0}(t) && (3.44)\\
P_{n,n}(t) &= (2n+1)uP_{n-1,n-1}(t) && (3.45)\\
P_{n,m}(t) &= P_{n-2,m}(t) - (2n-1)uP_{n-1,m-1}(t) && (3.46)
\end{aligned}
$$

In order to avoid some misleadings it is important to note that the notation $P_{n,m}$ is different from P_n^m, because they have a different sign in the generating function: they have same magnitude, but different sign when m is odd. In this work only the $P_{n,m}$ is used. The Legendre Polinomyal P_n are not the same things of associated Legendre functions $P_{n,m}$ and they correspond to the functions with degree n and order 0, so $P_{n,0}$. In some text instead of using the latitude φ it is used the colatitude $\pi/2 - \varphi$, that takes to a change of sign in the computation of derivatives. Spherical harmonics can be expressed also with the coefficients J_{nm}.

The J_2 coefficient is the most important and it is related to the bulge of the Earth at the equator. Along this thesis the model up to J8x8 harmonics is considered. The opposite gradient of the potential is the acceleration due to the asphericity of the Earth. Graphically the acceleration is perpendicular to the equipotential surface in the considered point.

$$\boldsymbol{a}_J = -\boldsymbol{\nabla}\Phi \tag{3.47}$$

That is, in scalar coordinates

$$
\begin{aligned}
(a_J)_u &= -\partial\Phi/\partial r && (3.48)\\
(a_J)_v &= -(\partial\Phi/\partial\vartheta)/(r\cos\varphi) && (3.49)\\
(a_J)_w &= -(\partial\Phi/\partial\varphi)/r && (3.50)
\end{aligned}
$$

So it is necessary to derive the potential (3.39). Differentiation with respect to r and ϑ is straightforward; while the derivatives with respect to φ require the derivatives of the associated Legendre functions, which are obtained recursively. Derivatives can be computed respect to the argument of the function or directly respect to φ. In the code implemented the second way is chosen. Posing $P_{nm} = 0$ if $m > n$

$$
\frac{\mathrm{d}P_{nm}}{\mathrm{d}\varphi} = \begin{cases} P_{n1} & \text{for} \quad m = 0 \\ [P_{n(m+1)} - (n+m)(n-m+1)P_{n(m-1)}]/2 & \text{for} \quad m > 0 \end{cases} \tag{3.51}
$$

Further details can be found in [61] and [62].

In order to shorten the equation, the following notation is introduced:

$$
\begin{aligned}
CcSsPs &= \sum_{m=0}^{n} \left(C_{nm}\cos m\lambda + S_{nm}\sin m\lambda\right) P_{nm}(\sin\varphi)\\
CsScPs &= \sum_{m=0}^{n} \left(-C_{nm}m\sin m\lambda + S_{nm}m\cos m\lambda\right) P_{nm}(\sin\varphi)\\
CcSsPC &= \sum_{m=0}^{n} \left(C_{nm}\cos m\lambda + S_{nm}\sin m\lambda\right) \frac{\mathrm{dP_{nm}}(\sin\varphi)}{\mathrm{d}\varphi}
\end{aligned} \tag{3.52}
$$

The derivatives of the potential are

$$
\begin{aligned}
\frac{\partial\Phi}{\partial r} &= \frac{\mu}{r^2}\Phi - \frac{\mu}{r}\left\{\sum_{n=2}^{N}(-n)\left(\frac{r_E}{r}\right)^n (CcSsPs)\right\} && (3.53)\\
\frac{\partial\Phi}{\partial\vartheta} &= -\frac{\mu}{r}\left\{\sum_{n=2}^{N}(-n)\left(\frac{r_E}{r}\right)^n (CsScPs)\right\} && (3.54)\\
\frac{\partial\Phi}{\partial\varphi} &= -\frac{\mu}{r}\left\{\sum_{n=2}^{N}(-n)\left(\frac{r_E}{r}\right)^n (CcSsPC)\right\} && (3.55)
\end{aligned}
$$

Once that the mathematical model is defined, the contribution of these perturbations to the Euler-Lagrange equations can be derived. For this purpose, also second derivative of the associated Legendre functions must be computed, but the scheme is the same as the first derivative. Geopotential perturbations, as all accelerations in the system dynamics, are involved in the computation of the Hamiltonian. The H_J term contains only the Earth asphericity acceleration, as written in Eq. (3.17) and (3.20)

$$H_J = \lambda_u (a_J)_u + \lambda_v (a_J)_v + \lambda_w (a_J)_w \tag{3.56}$$

and from this equation it is possible to write the contribution of geopotential perturbations $\dot{\boldsymbol{\lambda}}_J = -\partial H_J / \partial \boldsymbol{x}$ to the $\dot{\boldsymbol{\lambda}}$ differential equations

$$\begin{aligned}
(\dot{\lambda}_J)_r &= \lambda_u \left(\frac{\partial^2 \Phi}{\partial r^2} \right) + \lambda_v \left(-\frac{\mu}{r^2 \cos\varphi} \frac{\partial \Phi}{\partial \vartheta} + \frac{\mu}{r \cos\varphi} \frac{\partial^2 \Phi}{\partial r \partial \vartheta} \right) \\
&+ \lambda_w \left(-\frac{\mu}{r^2} \frac{\partial \Phi}{\partial \varphi} + \frac{\mu}{r} \frac{\partial^2 \Phi}{\partial \vartheta \partial r} \right) \qquad (3.57) \\
(\dot{\lambda}_J)_\vartheta &= \lambda_u \left(\frac{\partial^2 \Phi}{\partial r \partial \vartheta} \right) + \lambda_v \left(\frac{\mu}{r \cos\varphi} \frac{\partial^2 \Phi}{\partial \vartheta^2} \right) + \lambda_w \left(\frac{\mu}{r \cos\varphi} \frac{\partial^2 \Phi}{\partial \vartheta \partial \varphi} \right) \qquad (3.58) \\
(\dot{\lambda}_J)_\varphi &= \lambda_u \left(\frac{\partial^2 \Phi}{\partial r \partial \varphi} \right) + \lambda_v \left(\frac{\mu}{r \cos^2 \varphi} \sin\varphi \frac{\partial \Phi}{\partial \vartheta} + \frac{\mu}{r \cos\varphi} \frac{\partial^2 \Phi}{\partial \vartheta \partial \varphi} \right) \\
&+ \lambda_w \left(\frac{\mu}{r} \frac{\partial^2 \Phi}{\partial \varphi^2} \right) \qquad (3.59)
\end{aligned}$$

It is necessary to write the second derivative of Φ. In order to shorten the equations (and make them more comprensible) other functions are introduced

$$\begin{aligned}
m2CcSsPs &= \sum_{m=0}^{n} \left(-C_{nm} m^2 \cos m\lambda - S_{nm} m^2 \sin m\lambda \right) P_{nm}(\sin\varphi) \\
CsScPC &= \sum_{m=0}^{n} \left(-C_{nm} m \sin m\lambda + S_{nm} m \cos m\lambda \right) \frac{\mathrm{dP_{nm}}(\sin\varphi)}{\mathrm{d}\varphi} \\
CcSsP2 &= \sum_{m=0}^{n} \left(C_{nm} \cos m\lambda + S_{nm} \sin m\lambda \right) \frac{\mathrm{d^2P_{nm}}(\sin\varphi)}{\mathrm{d}\varphi^2} \qquad (3.60)
\end{aligned}$$

And now it is possible to write the second derivative of the potential.

$$\frac{\partial^2\Phi}{\partial r^2} = -2\frac{\mu}{r^3}\{1+\Phi\} + 2\frac{\mu}{r^2}\left\{\frac{\partial\Phi}{\partial r}\right\} - \frac{\mu}{r}\left\{\sum_{n=2}^{N} n(n+1)\left(\frac{r_E^n}{r^(n+2)}\right)(CcSsPs)\right\} \tag{3.61}$$

$$\frac{\partial^2\Phi}{\partial r\partial\vartheta} = \frac{\mu}{r^2}\frac{\partial\Phi}{\partial\vartheta} - \frac{\mu}{r}\left\{\sum_{n=2}^{N}(-n)\left(\frac{r_E^n}{r^(n+1)}\right)(CsScPs)\right\} \tag{3.62}$$

$$\frac{\partial^2\Phi}{\partial r\partial\varphi} = \frac{\mu}{r^2}\frac{\partial\Phi}{\partial\varphi} - \frac{\mu}{r}\left\{\sum_{n=2}^{N}(-n)\left(\frac{r_E^n}{r^(n+1)}\right)(CcSsPC)\right\} \tag{3.63}$$

$$\frac{\partial^2\Phi}{\partial\vartheta^2} = -\frac{\mu}{r}\left\{\sum_{n=2}^{N}\left(\frac{r_E}{r}\right)^n(m2CcSsPs)\right\} \tag{3.64}$$

$$\frac{\partial^2\Phi}{\partial\vartheta\partial\varphi} = -\frac{\mu}{r}\left\{\sum_{n=2}^{N}\left(\frac{r_E}{r}\right)^n(CsScPC)\right\} \tag{3.65}$$

$$\frac{\partial^2\Phi}{\partial\varphi^2} = -\frac{\mu}{r}\left\{\sum_{n=2}^{N}\left(\frac{r_E}{r}\right)^n(CcSsP2)\right\} \tag{3.66}$$

The method of writing the gravitational potential field by means of spherical harmonics is very precise, but it is also computationally demanding, especially when considering high fidelity optimization (200x200). In this case, also the use of recursive formulation, requires the most of computation power available. A new method have been proposed by Arora et al. [63], in which the gravitational field computed by harmonics is memorized and is interpolated by 3 degrees polynomial in a 3D mesh. In this way the operation of derivative is faster than the computation of the gravitational field. The two methods are comparable with a 10x10 degree, so in the case studied in this thesis the computation by harmonics is still faster

3.3 N-body perturbations

Asphericity of the central body is important when spacecraft is close to the central body, but if the artificial satellite is on an Highly Elliptic Orbit (HEO) the perturbations of other bodies influence trajectory and deployment strategy. When considering Earth as the central body the most important gravitational perturbations come from Moon and Sun. The position of the relevant bodies with respect to the Earth are evaluated using DE405 JPL ephemeris [64] [65] which provide the rectangular coordinates x_b, y_b, z_b in International Celestial Reference frame and

therefore in the EME2000. The differences between the two frames are very small and can be neglected in this problem. The subscript b stands for the generic perturbing body and is replaced by s for the Sun and l for the Moon. The perturbing acceleration has to be referred to the Earth reference system, so the force of the celestial body on the spacecraft and on the Earth should be computed and the difference represents the perturbing term. The relative distance Earth-Celestial Body is

$$\boldsymbol{r}_b = x_b \boldsymbol{I} + y_b \boldsymbol{J} + z_b \boldsymbol{K} \tag{3.67}$$

while the relative distance spacecraft-Earth is simply $\boldsymbol{r}$. The relative distance between the Spacecraft and the perturbing body is $\boldsymbol{R} = \boldsymbol{r} - \boldsymbol{r}_b$, as in figure 3.4. The perturbing acceleration is

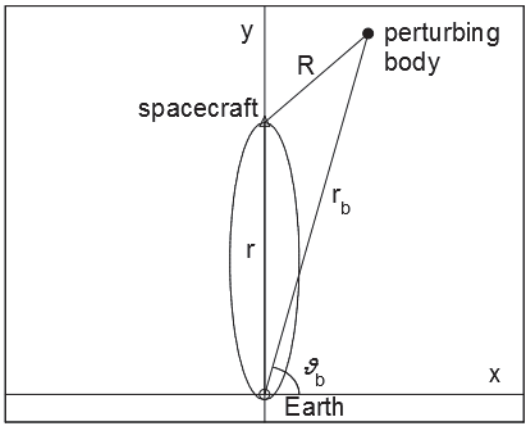

Figure 3.4: Schematic geometry of gravitational perturbations

$$\boldsymbol{a}_{bg} = \boldsymbol{a}_{b-sc} + \boldsymbol{a}_{b-E} = -(\mu_b/R^3)\boldsymbol{R} - (\mu_b/r_b^3)(\boldsymbol{r}_b) \tag{3.68}$$

In the topocentric reference frame one has

$$(a_{bg})_u = (\mu_b/R^3)[(r_b)_u - r] - (\mu_b/r_b^3)(r_b)_u \tag{3.69}$$
$$(a_{bg})_v = (\mu_b/R^3)(r_b)_v - (\mu_b/r_b^3)(r_b)_v \tag{3.70}$$
$$(a_{bg})_w = (\mu_b/R^3)(r_b)_w - (\mu_b/r_b^3)(r_b)_w \tag{3.71}$$

The vector $\boldsymbol{r}_b$ pointing from Earth to the perturbing Body has component

$$(r_b)_u = x_b \cos\vartheta \cos\varphi + y_b \sin\vartheta \cos\varphi + z_b \sin\varphi \tag{3.72}$$
$$(r_b)_v = -x_b \sin\vartheta + y_b \cos\vartheta \tag{3.73}$$
$$(r_b)_w = -x_b \cos\vartheta \sin\varphi - y_b \sin\vartheta \sin\varphi + z_b \cos\varphi \tag{3.74}$$

while the magnitude of R (the distance between the perturbing body and the spacecraft) is

$$R = \sqrt{[r - (r_b)_u]^2 + (r_b)_v^2 + (r_b)_w^2} \tag{3.75}$$

The gravity forces depends only on position and the perturbation forces are written in function of r, ϑ, φ and time t.

As for the perturbations of the asphericity of the Earth is concerned, the Hamiltonian terms which depend from the perturbation of another gravitational body, are introduced

$$H_{bg} = \lambda_u (a_{bg})_u + \lambda_v (a_{bg})_v + \lambda_w (a_{bg})_w \tag{3.76}$$

Now it is possible to compute the contribution to Euler-Lagrange equation

$$\begin{aligned}(\dot{\lambda}_{bg})_r = {} & \lambda_u \left(\frac{\partial (a_{b-sc})_u}{\partial r} + \frac{\partial (a_{b-E})_u}{\partial r} \right) + \lambda_v \left(\frac{\partial (a_{b-sc})_v}{\partial r} + \frac{\partial (a_{b-E})_v}{\partial r} \right) \\ & + \lambda_w \left(\frac{\partial (a_{b-sc})_w}{\partial r} + \frac{\partial (a_{b-E})_w}{\partial r} \right)\end{aligned} \tag{3.77}$$

$$\begin{aligned}(\dot{\lambda}_{bg})_\vartheta = {} & \lambda_u \left(\frac{\partial (a_{b-sc})_u}{\partial \vartheta} + \frac{\partial (a_{b-E})_u}{\partial \vartheta} \right) + \lambda_v \left(\frac{\partial (a_{b-sc})_v}{\partial \vartheta} + \frac{\partial (a_{b-E})_v}{\partial \vartheta} \right) \\ & + \lambda_w \left(\frac{\partial (a_{b-sc})_w}{\partial \vartheta} + \frac{\partial (a_{b-E})_w}{\partial \vartheta} \right)\end{aligned} \tag{3.78}$$

$$\begin{aligned}(\dot{\lambda}_{bg})_\varphi = {} & \lambda_u \left(\frac{\partial (a_{b-sc})_u}{\partial \varphi} + \frac{\partial (a_{b-E})_u}{\partial \varphi} \right) + \lambda_v \left(\frac{\partial (a_{b-sc})_v}{\partial \varphi} + \frac{\partial (a_{b-E})_v}{\partial \varphi} \right) \\ & + \lambda_w \left(\frac{\partial (a_{b-sc})_w}{\partial \varphi} + \frac{\partial (a_{b-E})_w}{\partial \varphi} \right)\end{aligned} \tag{3.79}$$

where the derivatives are

$$\frac{\partial (a_{b-sc})_u}{\partial r} = -\frac{\mu}{R^3} \left(-\frac{3}{R^2} (r - (r_b)_u)^2 + 1 \right) \tag{3.80}$$
$$\frac{\partial (a_{b-sc})_v}{\partial r} = -\frac{\mu}{R^3} \left(-\frac{3}{R^2} (r - (r_b)_u)(-(r_b)_v) \right) \tag{3.81}$$
$$\frac{\partial (a_{b-sc})_w}{\partial r} = -\frac{\mu}{R^3} \left(-\frac{3}{R^2} (r - (r_b)_u)(-(r_b)_w) \right) \tag{3.82}$$

$$\frac{\partial(a_{b-sc})_u}{\partial\vartheta} = -\frac{\mu}{R^3}\left(-\frac{3r}{R^2}\cos\varphi(-(r_b)_v)(r-(r_b)_u)+(-(r_b)_v)\cos\varphi\right) \quad (3.83)$$

$$\frac{\partial(a_{b-sc})_v}{\partial\vartheta} = -\frac{\mu}{R^3}\left(-\frac{3r}{R^2}\cos\varphi((r_b)_v)^2+(r_b)_u\cos\varphi-(r_b)_w)\sin\varphi\right) \quad (3.84)$$

$$\frac{\partial(a_{b-sc})_w}{\partial\vartheta} = -\frac{\mu}{R^3}\left(-\frac{3r}{R^2}\cos\varphi(-(r_b)_v)(-(r_b)_w)+((r_b)_v)\sin\varphi\right) \quad (3.85)$$

$$\frac{\partial(a_{b-sc})_u}{\partial\varphi} = -\frac{\mu}{R^3}\left(-\frac{3r}{R^2}(-(r_b)_w)(r-(r_b)_u)-(r_b)_w\right) \quad (3.86)$$

$$\frac{\partial(a_{b-sc})_v}{\partial\varphi} = -\frac{\mu}{R^3}\left(-\frac{3r}{R^2}(r_b)_w(r_b)_v\right) \quad (3.87)$$

$$\frac{\partial(a_{b-sc})_w}{\partial\varphi} = -\frac{\mu}{R^3}\left(-\frac{3r}{R^2}(r_b)_w^2+(r_b)_u\right) \quad (3.88)$$

$$\frac{\partial(a_{b-E})_u}{\partial r} = 0 \quad (3.89)$$

$$\frac{\partial(a_{b-E})_v}{\partial r} = 0 \quad (3.90)$$

$$\frac{\partial(a_{b-E})_w}{\partial r} = 0 \quad (3.91)$$

$$\frac{\partial(a_{b-E})_u}{\partial\vartheta} = -\frac{\mu}{r_b^3}\left((-(r_b)_v)\cos\varphi\right) \quad (3.92)$$

$$\frac{\partial(a_{b-E})_v}{\partial\vartheta} = -\frac{\mu}{r_b^3}\left((r_b)_u\cos\varphi-(r_b)_w)\sin\varphi\right) \quad (3.93)$$

$$\frac{\partial(a_{b-E})_w}{\partial\vartheta} = -\frac{\mu}{r_b^3}\left((r_b)_v\sin\varphi\right) \quad (3.94)$$

$$\frac{\partial(a_{b-E})_u}{\partial\varphi} = -\frac{\mu}{r_b^3}\left(-(r_b)_w\right) \quad (3.95)$$

$$\frac{\partial(a_{b-E})_v}{\partial\varphi} = 0 \quad (3.96)$$

$$\frac{\partial(a_{b-E})_w}{\partial\varphi} = -\frac{\mu}{r_b^3}\left((r_b)_u\right) \quad (3.97)$$

3.4 Solar Radiation pressure

Another perturbation that can be taken in account is the solar radiation pressure, that is the force which results from photons interacting with the spacecraft. The total power radiated by the Sun is $L_S = 3.84 \cdot 10^{26}\,\mathrm{W}$. The power is distributed on a sphere and so, going far from the Sun, the power for unit area decreases as the sphere surface increases. If c_{light} is the speed of light it is possible to write the solar radiation pressure as

$$p = L_S/(4\pi R^2 c_{light}) \tag{3.98}$$

where R is again the Spacecraft-Sun distance. At R^*=1 AU radiation pressure is $p^* = 4.55682 \cdot 10^{-6}\,\mathrm{N/m^2}$. Assuming reflectivity $\eta = 0.7$ the acceleration on a spherical body of mass m and cross-section S is

$$\boldsymbol{a}_{srp} = (1+\eta)p^*(R^*/R)^2(S/m)\boldsymbol{R}/R = \Gamma\boldsymbol{R}/(mR^3) \tag{3.99}$$

whose components are

$$(a_{srp})_u = \left[\Gamma/\left(mR^3\right)\right]\left[(r_s)_u - r\right] \tag{3.100}$$

$$(a_{srp})_v = \left[\Gamma/\left(mR^3\right)\right]\left[(r_s)_v\right] \tag{3.101}$$

$$(a_{srp})_w = \left[\Gamma/\left(mR^3\right)\right]\left[(r_s)_w\right] \tag{3.102}$$

The radiation pressure acts as a force in the Sun-Spacecrafts direction and it is inverse proportional to the squared distance of the two bodies. Therefore, the gravitational perturbation and the solar pressure radiation show the same dependence on distance and they are parallel but opposite. From the mathematical point of view the expression is the same as that of the gravitational perturbation, so they can be computed at the same time. The solar radiation term is computed as solar gravitational parameter modification in the force acting on the spacecraft (not on the Earth). The solar radiation pressure does not act on the spacecraft when Earth eclipses the Sun, so it is important to model the shadow. There are different type of model, such as the cylindrical shape, the conical one and different models of penumbra [66]. In the problem of transfer between elliptic orbits considered here the thruster is chemical, so the shadow does not influence the thrust and the radiation pressure perturbation is very small. The conical shadow seems the best approximation, without considering the most complex penumbra model. Issues regarding numerical instabilities due to the discontinuities in the solar radiation pressure have not been found. First step is to check if spacecraft and Sun are in opposite position with respect to the Earth. The relevant quantities are sketched (not to scale) in Fig. 3.5. If $(r_s)_u < 0$ then Sun is in the opposite side. If the penumbra is not considered, the Earth shadow cone has an angle of $\gamma_{shadow} = \sin^{-1}(r_E/r_s)$, where r_E is the Earth radius (only circular cone shadow is considered). To evaluate if

the spacecraft is inside or outside the shadow, the cone with axis on the Sun-Earth line, with center on the Sun and lateral surface tangential to spacecraft-Sun vector, is considered. The angle of the Sun-Spacecraft cone is $\gamma = \sin^{-1}(r \sin\delta / R)$, where δ is the angle centered on the Earth between $\boldsymbol{r}$ and $\boldsymbol{r}_s$ and it is evaluated as $\delta = \cos^{-1}[(r_s)_u / r_s]$. When $(r_s)_u < 0$ and $\gamma < \gamma_{shadow}$ the spacecraft is in the shadow of the Earth. The contribution to $\dot{\lambda}$ equation are the same as those of the N-Body gravitational perturbation and are evaluated in the same subroutine. The difference is that the acceleration depends on the instantaneous mass of the spacecraft and this fact introduces a new term in $\dot{\lambda}_m$ equation.

$$\Delta\dot{(\lambda_{spr})}_m = \frac{S \cdot C_s pr}{m^2} \frac{1}{R^3} \left(\lambda_u (r - (r_b)_u) + \lambda_v (-(r_b)_v) + \lambda_w (-(r_b)_w)\right) \tag{3.103}$$

where $S = 0$ if shadow is present.

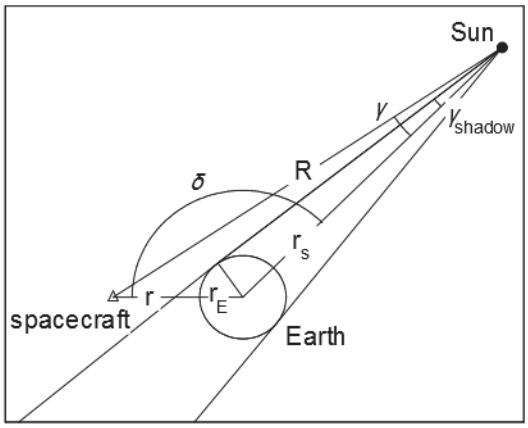

Figure 3.5: Schematic geometry of the Earth shadow

Conclusions

The chapter describes the two body model and introduces different perturbations: asphericity of the Earth, Moon and Sun gravity, Solar Radiation Pressure. The state variables differential equations are derived and Hamiltonian has been written in a local topocentric frame. The Hamiltonian has been used to derive the adjoint variables differential equations (Euler-Lagrange equations). Legendre associated functions and their derivatives are used for the computation of the geopotential perturbations. A conic shadow model without penumbra has been introduced for the solar radiation pressure perturbations.